Institute of Mathematical Geography

MONOGRAPHS

Essays on
Mathematical Geography
Volume III
Sandra Lach Arlinghaus
Monograph #14

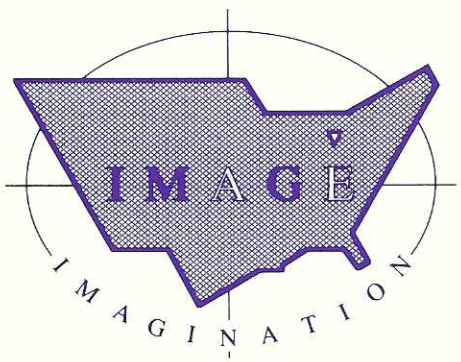

? IMaGe

ESSAYS ON MATHEMATICAL GEOGRAPHY — III

Sandra Lach Arlinghaus

June, 1991

Institute of Mathematical Geography

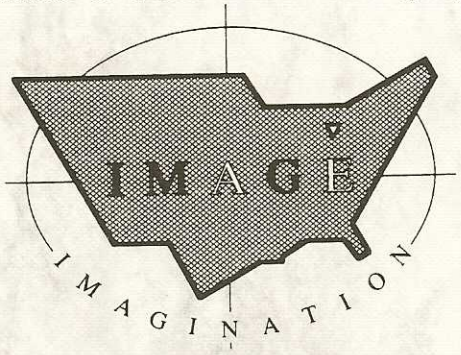

Monograph #14

Institute of Mathematical Geography
Ann Arbor, MI

TO

DAVID EDWARD VOORHEES ARLINGHAUS

on the occasion of his birth

June 7, 1991

Monographs published by the Institute of Mathematical Geography (IMaGe) 2790 Briarcliff St., Ann Arbor, MI, 48105, are printed by Digicopy, Inc., 1110 S. University Ave., Ann Arbor, MI 48104. They are printed on recycled, archival quality, paper, using a Xerox DocuTech which can scan original photos and figures directly into the text. The typesetting is prepared by IMaGe using TEX, the computerized typesetting program trademarked by Donald Knuth and the American Mathematical Society. IMaGe Monographs are refereed by professionals in mathematics and in geography—whatever is appropriate.

ISBN 1-877751-50-2

Volume III

AUTHOR'S PREFACE

This volume contains a series of essays, or attempts ("essayer," Fr.), to show how one might align various mathematical concepts with real-world situations. The point of demonstrating how alignment might be made, rather than showing only a finished product that can conceal how these associations are made, is to reveal the art in the process that can lead to science. In so doing, effort is made to bear in mind the importance of "the fit of ideas" [Mac Lane, 1982] — of craftsmanship in fitting mathematical tools to real-world settings that is critical in determining success.

These essays, some more complete than others, represent efforts at this process bridging a period of about twenty years. They follow in nature the two previous volumes of essays of this sort.

REFERENCE

Mac Lane, Saunders. "Proof, Truth, and Confusion." The 1982 Ryerson Lecture. The University of Chicago. Reprinted in *Solstice*, Winter, 1991, Ann Arbor: Institute of Mathematical Geography.

TABLE OF CONTENTS

CHAPTER 1

Table for Central Place Fractals

I. Introduction

Previous published research demonstrates how to use fractal [Mandelbrot, 1983, and elsewhere in reference to fractals] geometry to generate entire central place hierarchies, for arbitrary Löschian numbers, using a single fractal generator for an entire hierarchy [Arlinghaus, 1985; Arlinghaus and Arlinghaus, 1989]. Thus, it is assumed that the reader has seen or has access to material that will show at least the diagrams of how the classical $K = 3$, $K = 4$, and $K = 7$ hierarchies can be generated using fractal generators (Figure 1.1 suggests the procedure for the $K = 4$ central place hierarchy). When fractals are used, it is also possible to calculate how much space is filled by the net so created when the iteration is carried out as an infinite process.

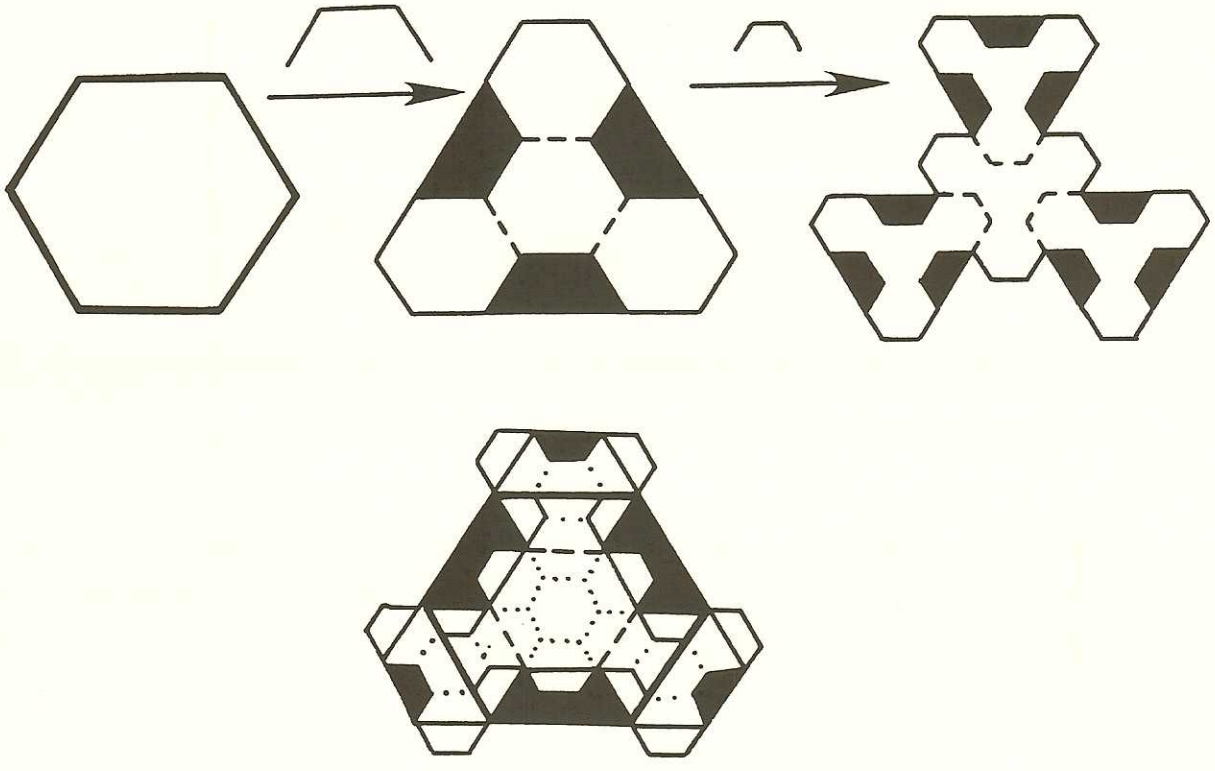

Figure 1.1. Fractal generation of the $K = 4$ central place hierarchy

Often, however, the mathematics behind the diagrams remains unseen by those who focus on diagrams in texts. This essay is an effort to represent the mathematical theorems as a "procedure" that can be stated in capsule form in a table.

II. Pattern of Central Place K-values

Central place K-values, as is well-known, measure the square of the distance between successive settlements of the same hierarchical level: with "distance" being measured as the number of units separating locations. The basic "unit" is the distance between adjacent points in a triangular lattice. Thus, it is convenient to coordinatize the triangular lattice using oblique axes with the x and y axes inclined at 60 degrees to one another. The line $y = x$ bisects the first quadrant at an angle of 30 degrees to either axis (Figure 1.2). Because the lattice points are at vertices of equilateral

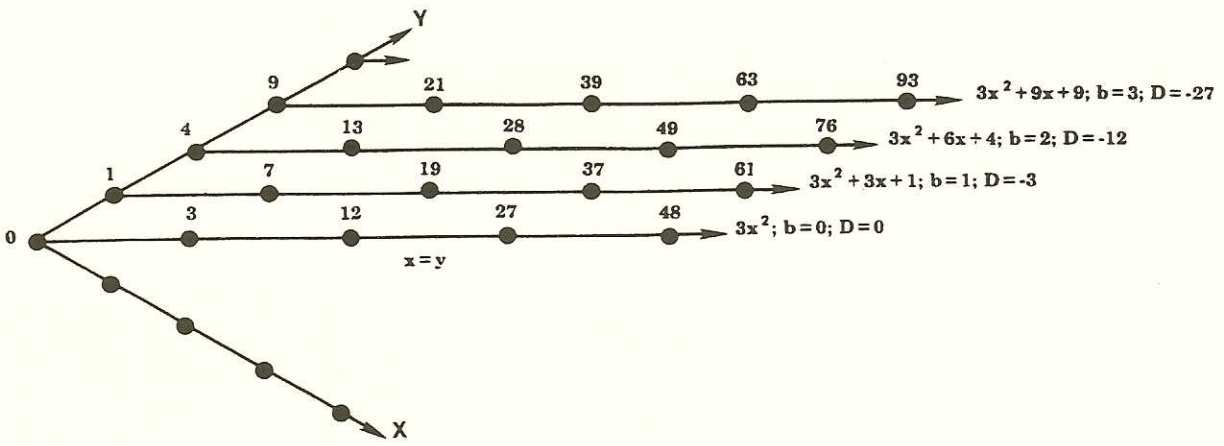

Figure 1.2. Triangular lattice showing two equations to generate entire point sets

triangles, it is evident that one way to partition the points in the lattice is by a series of lines parallel to the line $y = x$. When this is done, it is possible to characterize the set of K-values in a manner that is an alternate to Dacey's Diophantine equation

$$x^2 + xy + y^2 = K$$

that generates exactly the set of all K-values [Dacey, 1965]. The point to seeking an alternate algebraic expression is to use the second equation, together with the first, in order to solve

both equations for x and y, given K. Indeed, the equation

$$3x^2 + 3bx + b^2, \qquad b = 0, 1, \ldots, n$$

also generates exactly the set of all K-values [S. Arlinghaus, 1985, 1989]. It does so by partitioning the set into K-values that fall along lines parallel to $y = x$; when $b = 0$, the equation generates the K-values along the line $y = x$. When $b = 1$, the equation generates the K-values along the line translated one unit (in the appropriate direction) parallel to the line $y = x$. When $b = n$, the equation generates the K-values along the line translated n units (in the appropriate direction) parallel to the line $y = x$ (Figure 1.2). When the two sets of equations are used together, many of the "unsolved" problems in the geometry of central place theory yield solution [Arlinghaus and Arlinghaus, 1989].

For now, the latter equation is used to outline a procedure, derived from the theorem that produced that equation, that will permit the unique determination of the size and shape of a fractal generator for an arbitrary K. This unique determination is based only on the number-theoretic properties of the arbitrarily-selected value K.

III. Outline of Procedure.

K-values on the y-axis

To find the generator size and shape for any ordered pair on the y-axis, $(0, \sqrt{K})$, proceed as follows.

1. Find the equation of the line parallel to $y = x$ through $(0, \sqrt{K})$. It is:

$$3x^2 + 3\sqrt{K}x + (\sqrt{K})^2.$$

2. Find the discriminant, D, of this quadratic form:

$$D = (3\sqrt{K})^2 - 4 \cdot 3(\sqrt{K})^2 = -3K.$$

3. Find an integral value, j, as follows:

a. If $K \equiv 0 (\mathrm{mod}\, 3)$, then $j = \sqrt{K}/3$.

b. If $K \not\equiv 0 (\mathrm{mod}\, 3)$, then $j = (\sqrt{K} - 1)/3$ or $j = (\sqrt{K} - 2)/3$ whichever is an integer (clearly not both).

4. Table 1.1 then shows how to determine the number of fractal generator sides for an arbitrary K-value (determining whether or not an arbitrary integer is in fact a K-value–that

Table 1.1

K-value	Number of Generator Sides	Generator Shape — # of Hex-steps	
		$D \equiv 1 \bmod 4$	$D \equiv 0 \bmod 4$
$K \equiv 0 \bmod 3$	$2 + 4j$	$[\frac{2+4j}{2}]$	$[\frac{2+4j}{2}]$
$K \not\equiv 0 \bmod 3$			
j even	$3 + 4j$	$[\frac{3+4j}{2}]$	$[\frac{5+4j}{2}]$
j odd	$3 + 4j$	$[\frac{5+4j}{2}]$	$[\frac{3+4j}{2}]$

The brackets denote the greatest integer function.

is of the form $x^2 + xy + y^2$–is a separate matter (Arlinghaus and Arlinghaus, 1989). If the integer is congruent to $0 \bmod 3$ (evenly divisible by 3) then the number of generator sides is $2 + 4j$. Thus, for example, if $K = 36$, then by step 3a above, $j = \sqrt{K}/3 = 6/3 = 2$. Hence, the number of generator sides is $2 + 4 \cdot 2 = 10$. Suppose the integer is not congruent to $0 \bmod 3$. Whether or not the associated value of j is even or odd, the number of generator sides is $3 + 4j$. For example, if $K = 16$, $j = \frac{\sqrt{K}-1}{3} = \frac{4-1}{3} = 1$, from step 3 (note that $\frac{\sqrt{K}-2}{3} = 2/3$, not an integer as noted at the close of step 3 above). In this case, then, there are $3 + 4 \cdot 1 = 7$ sides in the fractal generator for a $K = 16$ hierarchy. Or, if $K = 64$, $j = \frac{\sqrt{K}-2}{3} = \frac{8-2}{3} = 2$ from step 3, so that there are $3 + 4 \cdot 2 = 11$ sides in the fractal generator for a $K = 64$ hierarchy. To determine the number of generator sides the parity of j does not matter; this will not be the case in determining generator shape. Table 1.2 shows j-values and number of fractal generator sides for a sample of K-values on the y-axis.

5. Table 1.1 also shows how to determine the generator shape. All that is required in addition to the number-theoretic properties of K (and related values, j and D) is the notion of a "hex-step." A hex-step is a step composed of two adjacent sides of a regular hexagon. All fractal generators are composed of hex-steps; typically, a generator has a rising sequence of hex-steps to a single edge plateau at the summit followed by a declining sequence of hex-steps. The question of shape then involves issues such as symmetry and whether or not the generator begins with a rise or a flat part of the hex-step. There are three basic configurations of hex-step patterns for generators associated with K-values on the y-axis.

a. The generator exhibits bilateral symmetry with respect to an axis perpendicular to the

Table 1.2

K-value		j-value					Number of Generator Sides	
$\equiv$ 0 mod 3	$\not\equiv$ 0 mod 3	$\equiv \frac{\sqrt{K}}{3}$	$\equiv \frac{(\sqrt{K}-1)}{3}$ even	odd	$\equiv \frac{(\sqrt{K}-2)}{3}$ even	odd	$\equiv$ 0 mod 3 $2+4j$	$\not\equiv$ 0 mod 3 $3+4j$
	4				0			3
9		1					6	
	16			1				7
	25					1		7
36		2					10	
	49		2					11
	64				2			11
81		3					14	
	100			3				15
	121					3		15
144		4					18	

generator plateau and bisecting the generator plateau. Such generators begin and end with a rise (Figure 1.3.a). The generator for the $K = 4$ hierarchy is the simplest of this sort.

b. The generator does not exhibit bilateral symmetry. There are two possibilites:

i. The generator begins on the left with a rising part of a hex-step in the rising sequence, and ends on the right with a tucked-under part so that the last element is a half-hexagon (Figure 1.3.b). The generator for the $K = 3$ hierarchy is the simplest of this sort; indeed, it is only a partial form of this type.

ii. The generator begins on the left with a flat part of a hex-step in the rising sequence, and ends on the right with a tucked-under part so that the last element is a half-hexagon (Figure 1.3.c). The generator for the $K = 7$ hierarchy is the simplest of this sort–again, a partial form of this type. For larger values, the structure is more fully revealed.

The generators for the classic $K = 3$, $K = 4$, and $K = 7$ hierarchies serve as a guide

Table 1.2, continued

		# of hex-steps — shape				
$D = -3K$		$K \equiv 0$	$K \not\equiv 0 \bmod 3$			
$\equiv$	$\equiv$		j even		j odd	
			$D \equiv 0$	$D \equiv 1$	$D \equiv 0$	$D \equiv 1$
$0 \bmod 4$	$1 \bmod 4$	$1 + 2j$	$\frac{(5+4j)}{2}$	$\frac{(3+4j)}{2}$	$\frac{(3+4j)}{2}$	$\frac{(5+4j)}{2}$
-12			2			
	-27	3				
-48					3	
	-75					4
-108		5				
	-147			5		
-192			6			
	-243	7				
-300					7	
	-363					8
-432		9				

to the basic form for any K value. In that regard, they serve as a "primitive" triple for underlying number-theoretic form, too.

The possibilities in a. and b. above occur as follows:

a. The case of bilateral symmetry occurs exactly when K is not congruent to $0 \bmod 3$ and

D is congruent to $0 \bmod 4$ and j is even

or (exclusive)

D is congruent to $1 \bmod 4$ and j is odd

The number of hex-steps in this case is $[\frac{5+4j}{2}]$. The brackets denote the greatest integer function ("floor" function).

b.

i. This case occurs when K is congruent to $0 \bmod 3$. In this case the number of hex-steps is $1 + 2j$.

ii. This case occurs exactly when K is not congruent to $0 \bmod 3$ and

D is congruent to $0 \bmod 4$ and j is odd

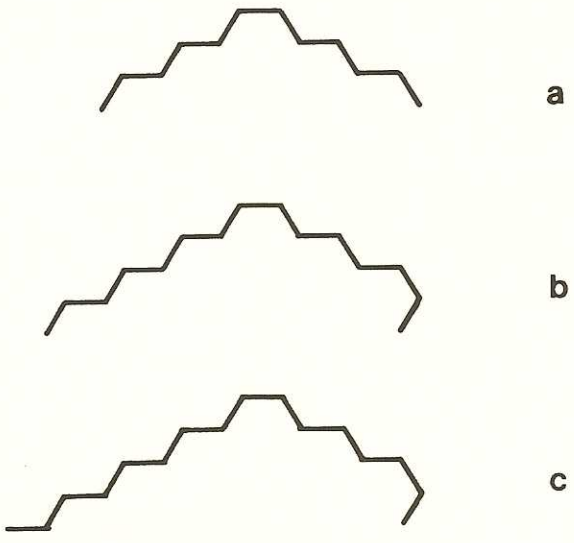

Figure 1.3. Three basic generator types: a. $K = 4$ type; b. $K = 3$ type; c. $K = 7$ type.

or (exclusive)

D is congruent to $1 \bmod 4$ and j is even

The number of hex-steps in this case is $[\frac{3+4j}{2}]$. The brackets denote the greatest integer function ("floor" function).

Thus, number-theoretic properties of K permit one to deduce the exact size and shape of a fractal generator needed to produce an entire central place hierarchy for an arbitrary K-value on the y-axis. Table 2 shows calculations associated with shape for a sample of y-axis K-values.

K-values not on the y-axis

Attached to each y-axis K-value is an infinite number of other K-values lying along a ray extending from a y-axis K-value parallel to the line $y = x$. These values satisfy exactly some equation of the form $3x^2 + 3bx + b^2$. To determine the size and shape of a fractal generator producing an entire central place hierarchy for a given K (not on the y-axis), **first**, find the y-axis entry corresponding to the chosen K and the fractal generator for this value;

then, determine the distance of K from the y-axis entry (as number of lattice points); and, **finally**, add, to the rising side of the y-axis generator one hex-step per unit of displacement from the y-axis.

Thus, for example, choose $K = 63$.

This value of K lies on the line $3x^2 + 9x + 9$ (and not on any other line of this form–see Arlinghaus and Arlinghaus, 1989). The y-axis entry is for $K = 9$. Extend the fractal generator of 6 sides for the $K = 9$ hierarchy–not bilaterally symmetric and beginning with a rise –by $3 \cdot 2$ sides (3 hex steps) on the rising side of the generator. Three hex-steps were used because 63 is the third lattice point over from the y-axis.

This simple extension means that for any K, the size and shape of the fractal generator can be completely determined using the number-theoretic properties of the situation — and, therefore, that the size and orientation of central place layers of hexagons are completely determined. The characterization therefore permits problems previously unsolved in the literature to be completely solved– such as Dacey's twin K-value problem and others (Arlinghaus and Arlinghaus, 1989). In addition, because the manner of characterization involves self-similarity, it is possible to calculate the fractal dimension for any central place hierarchy; what that dimension measures is how much the net fills space as the process is refined–as smaller and smaller hexagonal cells of the proper size and orientation are introduced. Thus, when the fractal dimension, F, is calculated as

$$F = \frac{\log n}{\log \sqrt{K}}$$

where n is the number of generator sides and K is the number of self-similar regions, it is an easy matter to calculate that for $K = 3$ the number n of generator sides is 2 and the number K of self-similar regions is 3 so that in this case $F = 1.262\ldots$. Similarly when $K = 4$, there are 4 self-similar regions and a fractal generator with 3 sides, so that $F = 1.585\ldots$, and when $K = 7$, there are 7 self-similar regions and a fractal generator with 3 sides, so that $F = 1.129\ldots$. Fractal dimensions for higher K values can be found readily as functions including values from a table like Table 1.1 that show how many sides are in a fractal generator associated with a given K.

Interpretations for what the fractal dimension might mean in a central place context are wide-ranging and, of course, subjective. In any interpretation, however, what that dimension *does* measure is the extent to which a plane region is filled by the lines of the given hierarchy

when the iteration is viewed as an infinite process. Of the three dimensions calculated above, the $K = 7$ hierarchy has the least space-filling associated with it, suggesting support for the classical subjective view of it as being organized along an "administrative" principle in which boundaries of high-order central place market areas do not subdivide the central places next lower in the hierarchy; high order central places retain control over their own bailiwick.

REFERENCES

Arlinghaus, S. L. Fractals take a central place, *Geografiska Annaler*, 67B, 83-88, 1985.

Arlinghaus, S. L. and Arlinghaus, W. C. Fractal theory of central place geometry: A Diophantine analysis of fractal generators for arbitrary Löschian numbers. *Geographical Analysis* . 21:103-121. 1989.

Dacey, M. F. The Geometry of Central Place Theory. *Geografiska Annaler*, 47, 111-24. 1965.

Mandelbrot, B. F. *The Fractal Geometry of Nature*. San Francisco: W. H. Freeman. 1983.

CHAPTER 2 *

Tiling According to the "Administrative" Principle

I. Introduction

The creation of central place hierarchies using a fractal generator is achieved by using a single generator, suitably scaled, to produce self-similar regions at various scales. Thus, for example, the "linear" broken-line generator of four segments of equal length produces the $K = 7$ hierarchy (Figure 2.1).

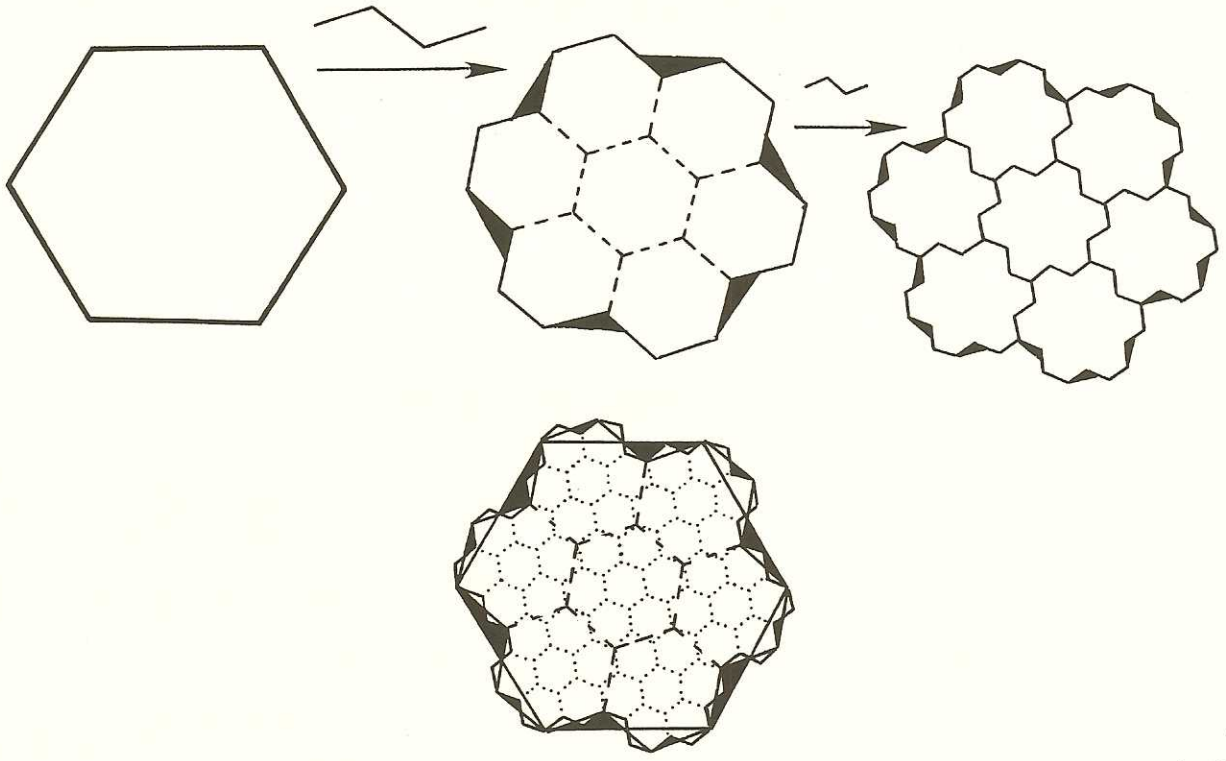

Figure 2.1. Fractal generator for a $K = 7$ hierarchy

The fractal strategy permits the calculation of the extent to which the boundary fills a plane region as the iteration is allowed to become infinite [Mandelbrot, 1983] (and elsewhere in reference to fractals). One might, however, view the creation of these central place patterns as a matter of tiling, or "patterning," the plane with suitably shaped boundary pieces. If the broken-line fractal generator were chosen as a boundary pattern, rules for placing it in the

plane, that would generate the $K = 7$ pattern could be specified but because of the "linear" nature of the shape, the set of rules would necessarily be more complicated than would the fractal iteration. Instead, it is possible to choose as a pattern, rather than as a fractal generator, a piece of a different shape that is not homeomorphic to the fractal generator. The pattern generator, itself, "fills" more space than does the corresponding fractal generator; the pattern generator for $K = 7$ is a three-armed star (3-stars, from an underlying triangular grid). When 3-stars are hooked together, a net of hexagons arises (Figure 2.2).

When suitably-scaled 3-stars are also hooked together and then superimposed on the larger hexagons, two layers of the $K = 7$ hierarchy emerge (Figure 2.3).

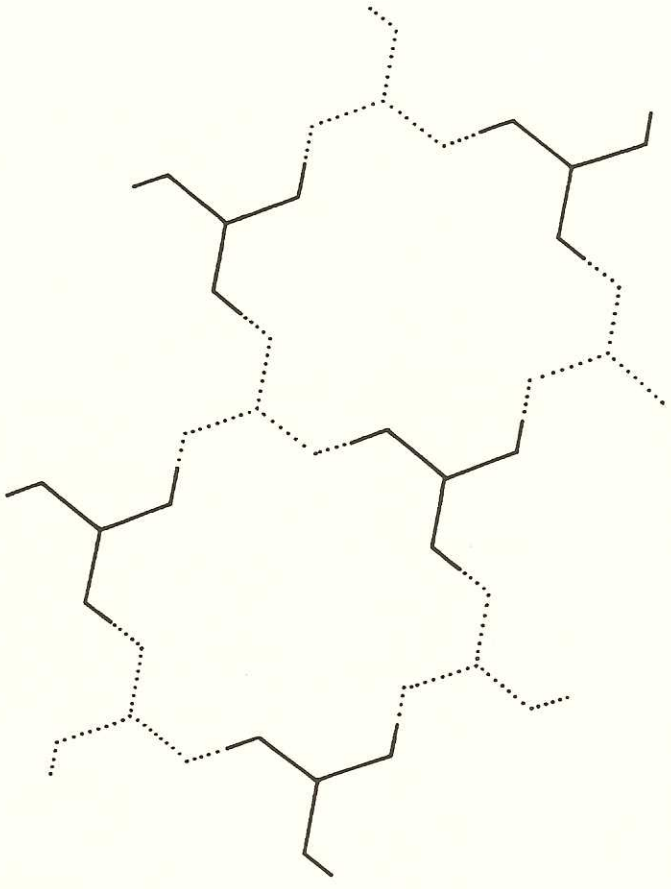

Figure 2.2. Single layer of 3-stars

Indeed, using this pattern-piece generates all the lines of a $K = 7$ hierarchy, as a net traced out by the arms of these 3-star "spiders" hooked arm-to-arm forming ranks to cover the plane in an unambiguous manner, with smaller spiders hanging off every bend and endpoint

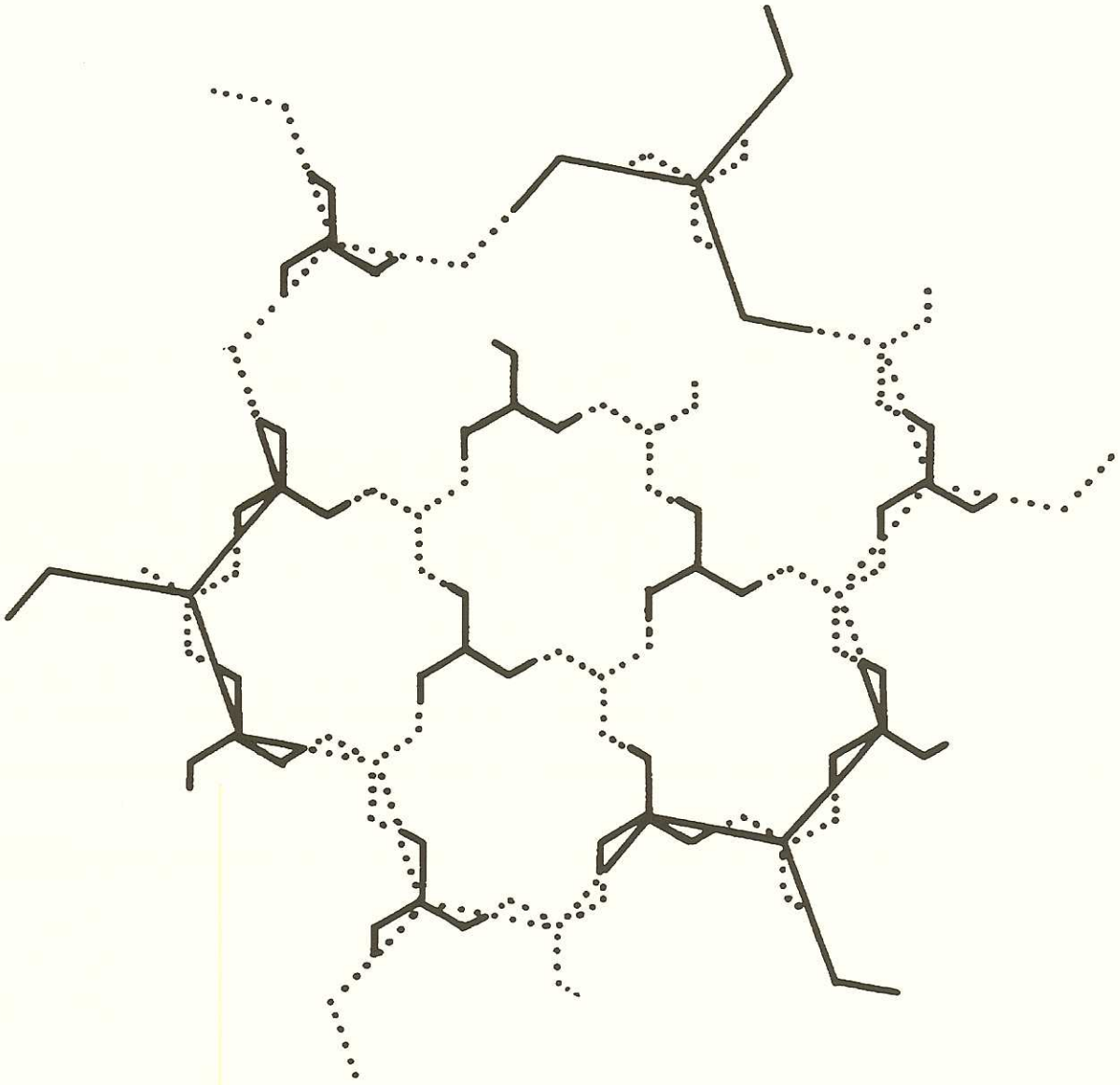

Figure 2.3. Layers of 3-stars produce $K = 7$ layering

of its larger counterpart (as do the young of so-called hanging "spider" plants). Thus, an alternate method of generating the $K = 7$ hierarchy from self-similar pieces provides extra detail; when all lines are present, the boundary will fill a two-dimensional piece of space. Thus, the strictly fractally-generated hierarchy (of Figure 2.1), of fractal dimension

(1.1291501 in this case), provides a skeletal structure on which to hang the rest of the detail (Figure 2.3).

II. A $K = 7$ Tiling on a Square Grid

There are, of course, an infinite number of tilings and patterns that one might produce in the plane [Grünbaum and Shephard, 1987]. A natural next step is to attempt to extend the ideas of fractal generation of central place hierarchies in various directions, including in that of using underlying plane tilings other than the equilateral triangle.

Consider an underlying grid composed of squares. Create the corresponding fractal "$K = 7$" construction using a square initiator (instead of an hexagonal initiator) and a generator composed of four segments of equal length, arranged in a zig-zag pattern with one maximum and one minimum, scaled to fit the initiator. Figure 2.4 shows such a configuration. When the generator is applied successively to each of the four sides of the initiator, the resulting boundary shape contains the equivalent of eight self-similar copies of the previous stage (a square) (Figure 2.4b). Scaling the generator and applying it successively to each side of Figure 2.4b produces Figure 2.4c containing the equivalent of eight regions self-similar to Figure 2.4b. This sort of "interlocking cross" pattern is similar, but not identical, to some of the base grids from which Escher designed intricate patterns of birds in flight emerging from backgrounds of fields [Schattschneider, 1990].

This construction produces an iteration of eight (rather than 7) self-similar new regions each time. Thus, when the fractal dimension D measuring the extent to which a boundary fills space when the iteration is carried out indefinitely, is calculated as

$$D = \frac{\log n}{\log \sqrt{K}}$$

if follows that for the construction suggested in Figure 2.4, $D = \frac{\log 4}{\log \sqrt{8}} = \frac{4}{3} = 1.33\ldots$. Thus, the boundary fills more space than does the corresponding construction using a hexagon as an initiator on an underlying triangular lattice. Again, the fractal construction gives the skeletal form of the hierarchy; greater detail may once again be systematically created as a construction similar to that afforded by the 3-stars above.

A four-armed star (4-star–familiar geometric ornament found adorning Greek pottery, Amerindian art, and Third Reich flags (in orientation opposite to the Amerindian) [Encyclopedia Britannica, 1967]) can be placed in evenly-aligned rows and columns to cover an entire plane region (Figure 2.5); such placement also outlines a set of first teragons (as suggested

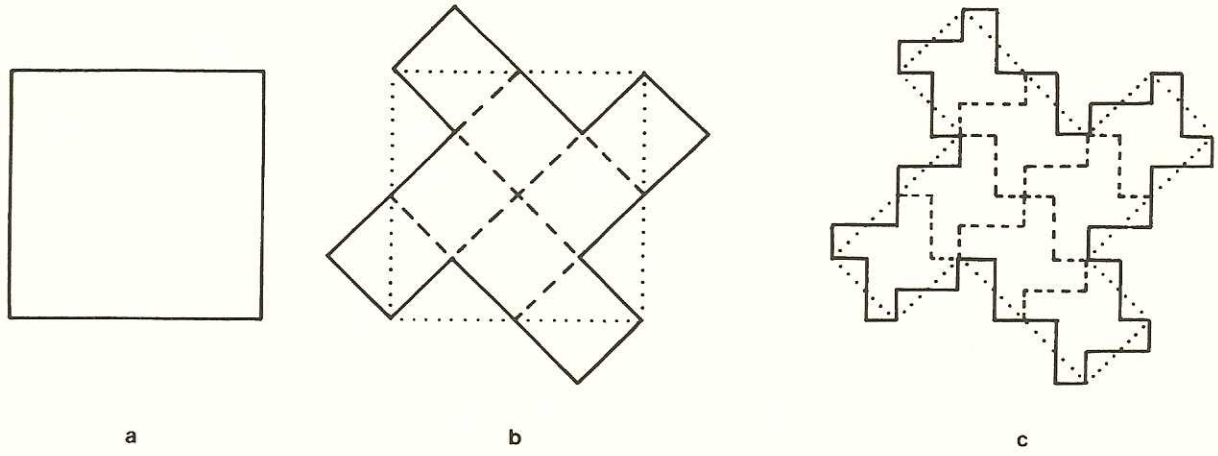

Figure 2.4. Fractally-generated square tiling sequence. a. Square initiator. b. First teragon formed by applying generator to initiator–it contains eight self-similar copies of the previous stage. c. Second teragon formed by applying scaled generator to first teragon–it contains eight self-similar copies of the previous stage.

by the shading of one in Figure 2.5). Further, when an added 4-star (dotted in Figure 2.5) is introduced within each teragon, in the only possible way, the detail of the tiling is produced. Iteration of this technique, hanging suitably-scaled 4-stars from every bend and endpoint of larger 4-stars, produces successive layers in the corresponding hierarchy (Figure 2.6). As in the case with the underlying triangular lattice, the fractal iteration on a square lattice permits measuring how much of the plane will be filled by a skeleton of a hierarchy; the iteration by stars introduces extra detail suggested by the fractal iteration.

III. Fractal dimensions

It is an easy matter to consider fractal constructions for counterparts to the $K = 3$ and $K = 4$ constructions on a square lattice–in both cases, they are uninteresting and even the simple skeletal boundary is space-filling. Thus, only the $K = 7$ case was displayed in the previous section. Higher values should also be non-trivial and are a topic for future

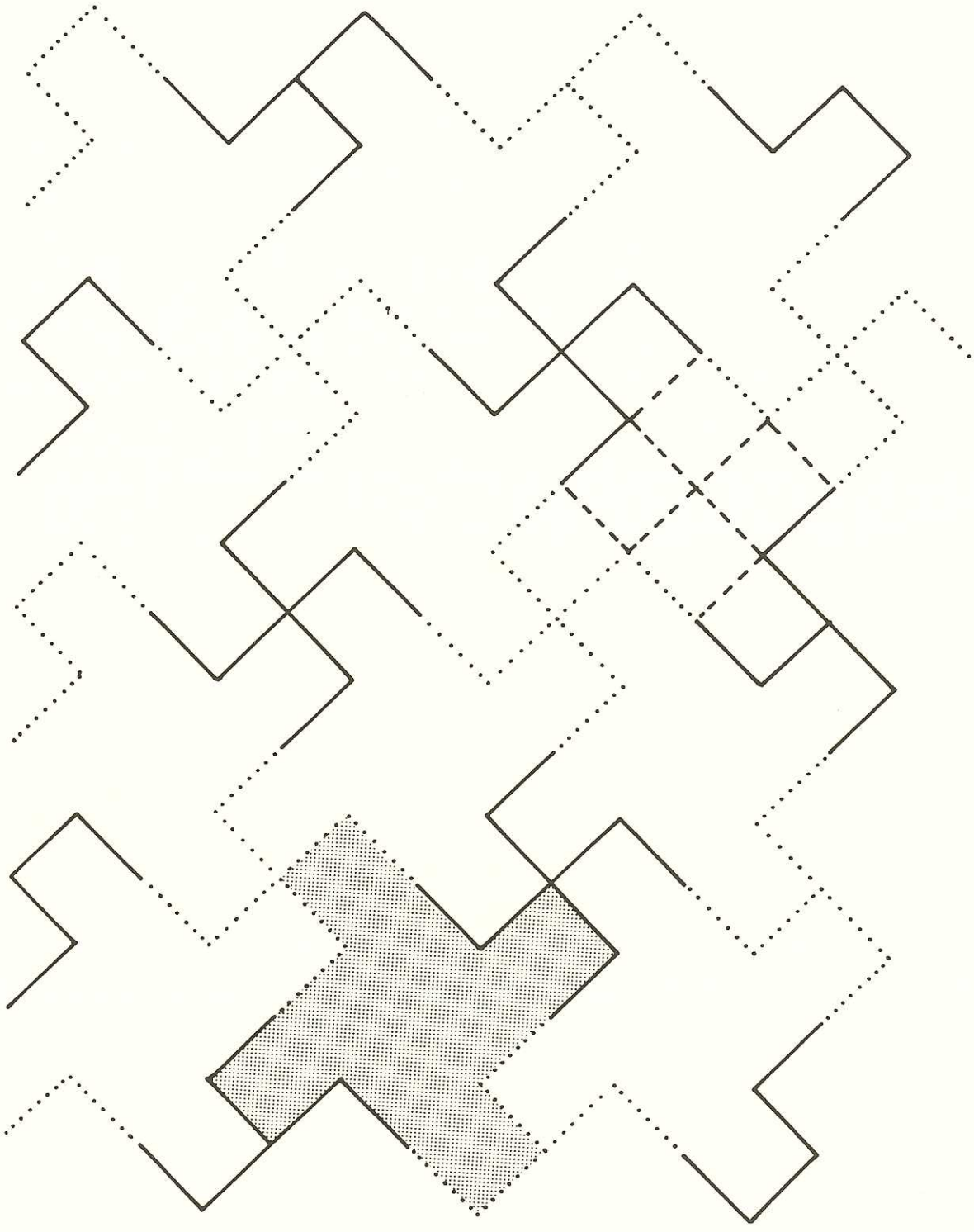

Figure 2.5. 4-stars used to cover a plane region; shading shows that they surround first teragons from Figure 2.4

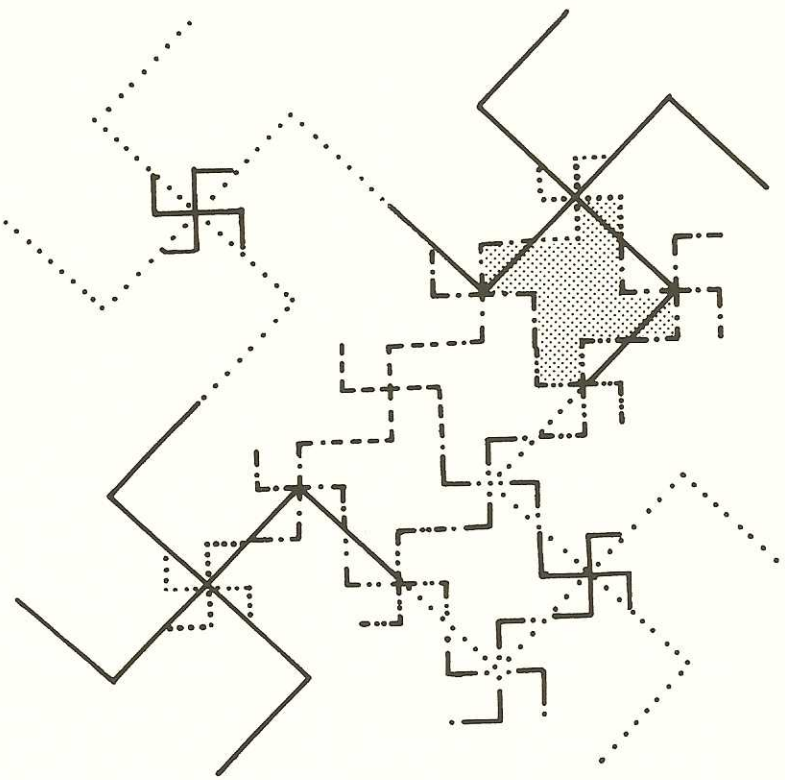

Figure 2.6. Scaled 4-stars used to create a hierarchy corresponding to the fractally-generated one of Figure 2.4; shaded region suggests a second teragon (Figure 2.4c)

effort; here, the $K = 7$ counterpart was focused on because it was the first one of interesting geometric structure.

Fractal dimensions permit comparisons between a $K = 7$ hierarchy of hexagons and a $K = 7$-like hierarchy of squares–the former of dimension $1.1291501\ldots$ and the latter of dimension $1.33\ldots$. One reason for being interested in making such a comparison might arise in an electronic environment. Squares are the fundamental picture element (pixel) currently employed; there has been considerable discussion as to the merits of using an hexagonal pixel, instead (as the optimum close-packing). Without considering important issues that involve printer construction and changing of existing technology, the fractal dimension alone can offer some insight involving differences in pixel shapes (which might then be used in conjunction with other issues). Layers in the sort of geometric hierarchy of squares and

hexagons suggested in Figures 2.4 and 2.1 represent the idea of increasing the resolution on a cathode ray tube (crt). Thus, suppose that the size of a square pixel on a crt is that of the square in Figure 2.4a. To see better a segment of the crt, one might increase the number of cells on the crt so that more detail can be seen; the method of doing this is to increase the pixel number by lines parallel to the sides of the previous network. Because content is carried on the pixel interiors, and not on the pixel boundary, and because the method of improving picture definition is one that is space-filling (totally filled by boundary), there is a point of diminishing returns in refining pixel size to increase picture definition. At least, this is the case when such refinement is done in a space-filling manner. When it is not, in which case new, finer nets are twisted relative to the background of older nets, the skeletal boundary does not fill two dimensions. Thus, increasing the number of pixels, when done with regard for space-filling characteristics of the pixel boundaries, can offer continually improved picture definition. When squares are used in this manner, the $K = 7$-like construction works in this regard; however, when the actual $K = 7$ construction, with hexagonal pixels, is used, there is even less filling with boundary so that, in this regard, the hexagonal pixel construction is superior to that using the square. So, one direction for application of this material is in an electronic environment [Arlinghaus, 1990]; another might be in site selection for locally unwanted land uses.

Landfills, management of toxic or radioactive wastes, and other land uses that are generally perceived as locally undesirable are also landuses that benefit from some sort of cohesive (rather than divided) central administrative control in order to avoid turf wars based on whose "back yard" is being infringed upon. Thus, one might consider placing unwanted land uses in a central position within a configuration relatively unfilled by boundary; the more a region is filled by boundary the more likely the boundary is to interfere. Thus, a $K = 7$ orientation for a hierarchy of increasingly fine land subdivisions suggests placing unwanted uses at the centers of the snowflake-like teragons, independent of scale. Indeed, the hierarchy, which reflects change in scale of the unwanted use corresponds to change in land parcel area as one moves from rural to urban: a suburban home generally sits on a "field" smaller than does a farmhouse, and a central city home generally sits on a "field" smaller than does a suburban home. This obvious and well-known rural/urban scale-change fits well with the corresponding scale change in the geometric hierarchy; it is appropriate to draw on this fit when locating unwanted landuses is important, because they too exhibit the same scale phe-

nomenon. Now much of our land survey and our street system is laid out along rectangular axes; thus, the hierarchy depicted in Figures 5 and 6 might be of greater actual use in siting locally unwanted land uses than would that of Figure 1, even though the fractal dimension of 1.1291501 for the hexagonal layout indicates that the likelihood of crossing a boundary is 56.5% while in the corresponding square layout the fractal dimension is 1.33 so that the boundary-crossing likelihood is higher at 66.7%. One would have to consider if the trade-off between having the geometry "fit" the parcel shape was worth an increased likelihood of split control–again, choosing the proper abstract tool to fit the real-world circumstance is critical.

REFERENCES

Encyclopedia Britannica, "Swastika." 1967.

Mandelbrot, B. F. *The Fractal Geometry of Nature.* San Francisco: W. H. Freeman. 1983.

Schattschneider, D. *Visions of Symmetry: Notebooks, Periodic Drawings, and Related Works of M. C. Escher*, New York: W. H. Freeman, 1990.

* Based in part on a lecture given in the Department of English, Visiting Writer Workshop in Composition, University of Michigan, 1990.

CHAPTER 3

Moiré Maps

Usually one thinks of finding Moiré patterns in broad expanses of silken fabric; as the material folds softly in the light, ripples of pattern give the silk an appearance of pools of darker and lighter color. Indeed, rippled patterns that produce a wavy appearance in the underlying material are not limited to cloth; they might equally appear in maps, under certain conditions.

Elementary laboratory courses in Physics often demonstrate quite aptly that the pattern of waves in a ripple tank can be altered by changing the boundaries of the margins and interior of the tank. A geographic pattern of ripples will also be governed by the "tank" or region that contains them. Basin shape influences ripple pattern.

The following example arose in considering congestion along arterials in Ann Arbor that have bus routes.

1. Designate points of heavy concentration of bus use; typically, these include hospitals, shopping malls, large educational institutions, and the central bus terminus. Each of these locations will have a weight assigned to it, based on the number of possible transfers available at a given location. Thus, if three different routes enter a given location, there are six possible buses, three inbound and three outbound from which a passenger might choose. Because the passenger can at most go from one bus to another (not backing up on the same route number), the number of possible transfers is to four other buses–inbound and outbound on two other routes; thus, there are 6 times 4 possibilities. Generally, if there are n distinct routes (counting inbound and outbound as separate routes) at a stop that is not the central terminus then there are n times $n-2$ possible transfers at that location; at the central terminus, there are n times $n-1$ possible transfers (Table 3.1). Thus, a location served by three different route lines (inbound and outbound) would be assigned a "transfer" weight of 24. More generally, what is required is to be able to weight designated locations in some consistent manner that is based on whatever real-world issue is under consideration–in this case, congestion and the movement of people [see also, for other related material, Arlinghaus and Nystuen, 1989].

Table 3.1 shows a set of distinguished locations in Ann Arbor each assigned a transfer weight based on how many bus lines pass through each.

Table 3.1, based on 1985 data

Location	# of bus routes	Transfer weight
1. Westgate Shopping Mall	Two	$4 \cdot 2 = 8$
2. Pioneer High School	Three	$6 \cdot 4 = 24$
3. University of Michigan, central campus	Three	$6 \cdot 4 = 24$
4. University of Michigan, athletic campus	Three	$6 \cdot 4 = 24$
5. Briarwood Mall	Three	$6 \cdot 4 = 24$
6. Arborland Mall	Two	$4 \cdot 2 = 8$
7. Packard Road Shopping	Two	$4 \cdot 2 = 8$
8. Meier's Shopping	Two	$4 \cdot 2 = 8$
9. Central bus terminus	Twelve	$12 \cdot 11 = 132$
10. Broadway shopping	Three	$6 \cdot 4 = 24$
11. University of Michigan hospital	Three	$6 \cdot 4 = 24$
12. Veterans' Administration Hospital	Three	$6 \cdot 4 = 24$
13. Huron High School	Two	$4 \cdot 2 = 8$
14. University of Michigan, north campus	Two	$4 \cdot 2 = 8$
15. Plymouth Road Mall	Two	$4 \cdot 2 = 8$
16. Plymouth Green Mall	Two	$4 \cdot 2 = 8$
17. Washtenaw Community College	Two	$4 \cdot 2 = 8$
18. St. Joseph Hospital	One	$2 \cdot 0 = 0$
19. Ypsilanti High School	One	$2 \cdot 0 = 0$
20. Eastern Michigan University	Three	$6 \cdot 4 = 24$
21. Ypsilanti terminus	Three	$6 \cdot 4 = 24$
22. Ypsilanti shopping area	Two	$4 \cdot 2 = 8$
23. Beyer Hospital	Two	$4 \cdot 2 = 8$
24. Willow Run High School	One	$2 \cdot 0 = 0$

2. Using the locations from 1 a consistent procedure, based in part on transfer weights and the balance of load between adjacent transfer points and in part on local transit demands and similar factors, was used to create basins surrounding each transfer point (Map 3.1). This sort of map is a common tool—polygons partition the plane forming service regions of some sort. What was **not** involved in determining the polygon placement was the Euclidean distance from a transfer point.

3. Contour the surface within each region, using some yardstick for determining contour interval that remains constant throughout the map and that was **not** used in basin formation. Here, each basin was contoured using Euclidean distance into thirds, measured from each transfer point, into sub-basins with the edges parallel to the basin margin. This sort of partition was chosen to reflect the relatively regular designation by the Ann Arbor Transportation Authority of "time points" along each route, for which published times are announced (but not for stops in between time points). When this procedure was executed, the map in Figure 3.2 was the result.

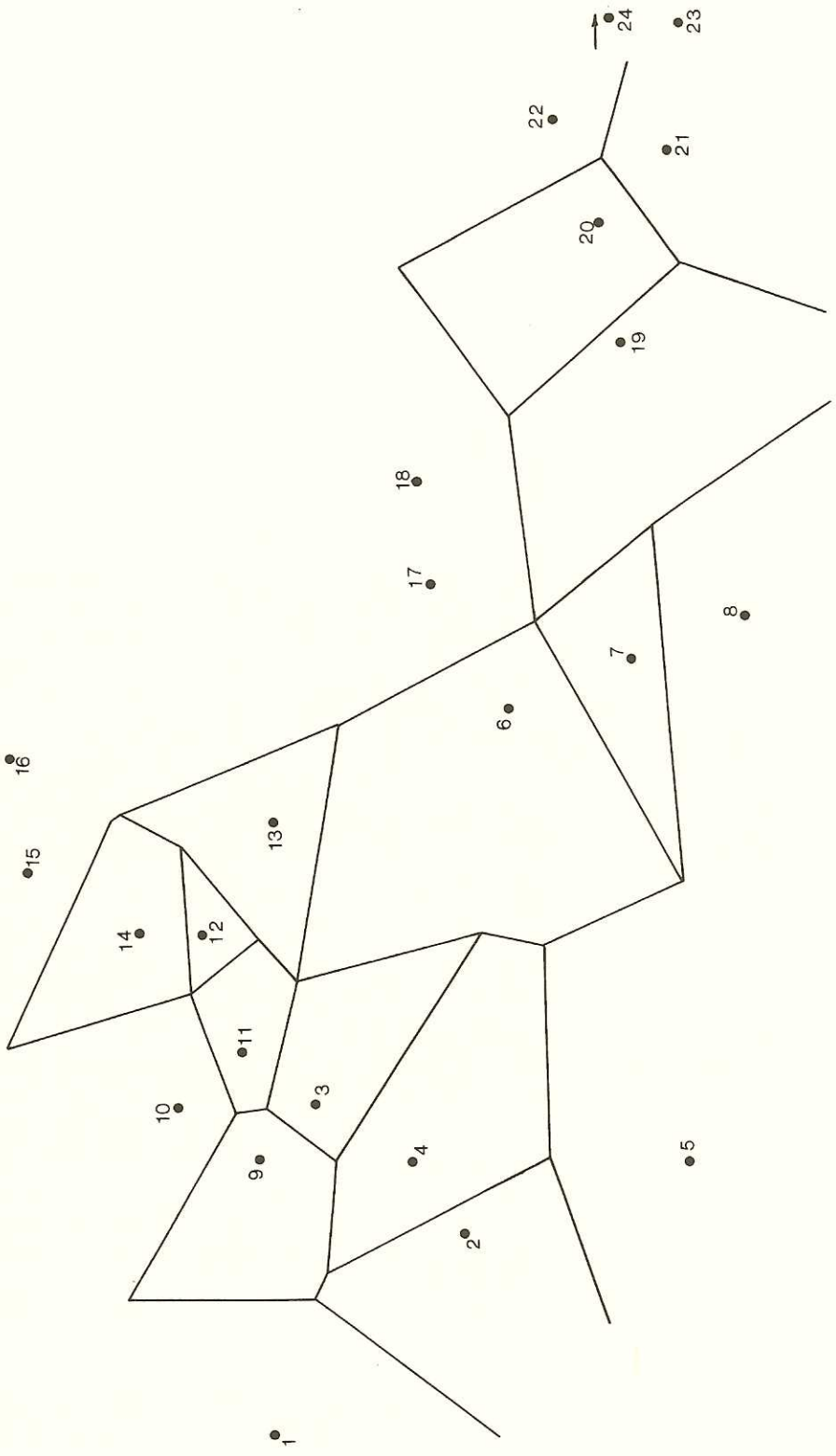

Figure 3.1. Basins surrounding bus transfer points — Ann Arbor/Ypsilanti, 1985. Numerals refer to left hand column of Table 3.1

When the method of contouring the regional basins has to do with the process underlying the partition into basins (as in this case), basin shape influences ripple pattern. When a different measure is superimposed, in a way that plays "across" the underlying grain of the basins, the effect is a Moiré pattern. In the Moiré map of Figure 3.2, the tight contour lines suggest "folds" in the underlying surface bounding pools of heavy bus passenger congestion.

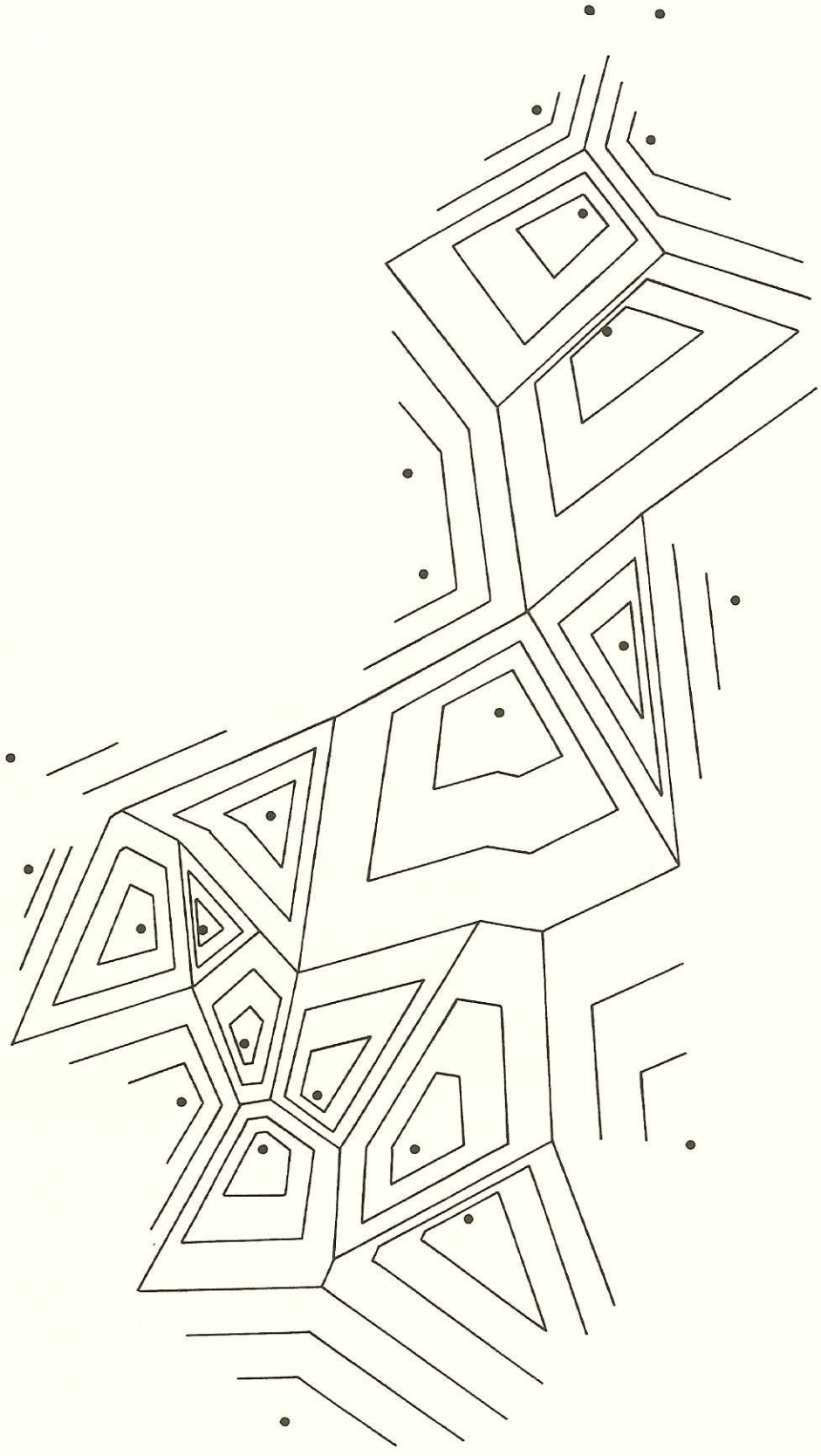

Figure 3.2. A Moiré Map surrounding bus transfer points

REFERENCES

Arlinghaus, S. and Nystuen, J. *Environmental Effects on Bus Durability*, Institute of Mathematical Geography, 1989.

CHAPTER 4 *

Triangle Partitioning

To partition a triangular cell $(V_1V_2V_3)$ into subtriangles with common vertex P_A, in which each subtriangle contains an assigned percentage of the areal, perimetric or angular measure of the entire cell $(V_1V_2V_3)$ (Figure 4.1), is geometrically straightforward. The interest in exhibiting the details of these constructions lies in drawing together fundamental geometric and geographic ideas to form a foundation from which further exploration of more complex geographical problems may proceed.

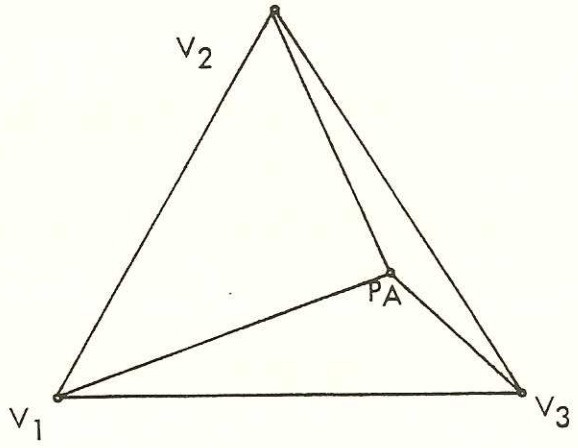

Figure 4.1

Area, perimeter, and angle, basic concepts familiar from Euclidean geometry, have natural geographic counterparts in area, boundary, and direction. Although formal procedure will be presented to partition a triangle with respect to each of area, perimeter, and angle, only partition with respect to perimeter will be developed.

A boundary (perimeter) separates an area into two distinct areas (assuming that it does not cross itself; that is, that it is a Jordan curve). Or, a boundary belongs to exactly one of the two areas it separates. Or, a boundary between two areas consists of all elements common to both areas. That is, a boundary is both a barrier to and transmitter of movement. This view of a boundary suggests that formal partitioning of a geometrically simple area such as a triangle might be extended to be of use in a geographically more complex region, for locating

transportation and communication networks, for they also are barriers to and transmitters of movement.

Partition with respect to area

The following construction presents a method of partitioning a triangle $(V_1V_2V_3)$ of area A into three subtriangles $V_{x_1}, V_{x_2}, V_{x_3}$ with a common vertex, P_A, such that the area $V_{x_i} = X_iA/100, \quad i = 1, 2, 3$ (Figure 4.2). The X_i are preassigned percentages with $\sum_{i=1}^{i=3} X_i = 100$

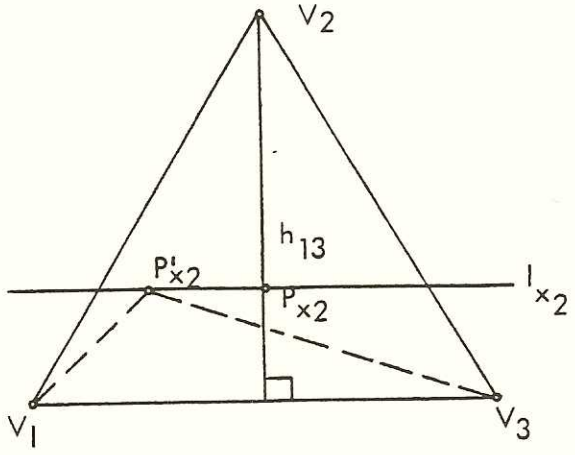

Figure 4.2

Existence of P_A

Let h_{13} denote the altitude of $\Delta V_1V_2V_3$ from V_2 (Figure 4.3).

Then $A = (h_{13}|V_1V_3|)/2$. Locate a point P_{x_2} on h_{13} such that

$$d(P_{x_2}, (V_1V_3)) = (X_2/100)h_{13}$$

where this length is measured from $V_1V_3 \wedge h_{13}$. Thus $\Delta V_1P_{x_2}V_3$ contains $X_2\%$ of A since

$$\text{area of}\Delta V_1P_{x_2}V_3 = (1/2|V_1V_3|)(h_{13}(X_2/100)) = A(X_2/100),$$

which will be labelled as A_{x_2}. The locus of points such that V_1V_3 and A_{x_2} are constant is a straight line l_{x_2} (Figure 4.2) through P_{x_2} parallel to V_1V_3. The line l_{x_2} must contain the desired point P_A. For, if P_{x_2} is any point on l_{x_2}, clearly the two triangles $(V_1V_3P_{x_2})$ and $(V_1V_3P'_{x_2})$ have the same area, A_{x_2}, since they have the same altitude and identical

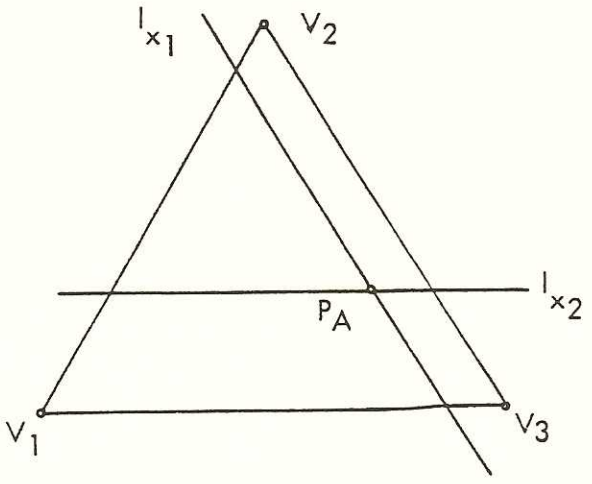

Figure 4.3

base. A similar construction will yield a point P_{x_1} and a line l_{x_1} associated with it such that $l_{x_1} \| V_2V_3$. Since P_A must also lie on l_{x_1}, the intersection $l_{x_2} \wedge l_{x_1}$ must produce a point P_A (Figure 4.3) satisfying the original conditions (the symbol '$\wedge$' denotes the intersection of two geometric entities). This reasoning is not valid in an arbitrary space; two lines must intersect in exactly one point.

Enumeration possibilities for P_A

Suppose $l_{x_2} \| V_1V_3$ and suppose $l_{x_1} \| V_2V_3$ with $l_{x_1} \wedge l_{x_2}$ producing a P_A. If instead, l_{x_3} had been chosen such that $l_{x_3} \| V_2V_3$, a new point $P_A{}'$ would be produced that satisfied the requirements of the problem, provided $X_3 \neq X_1$. (If $X_3 = X_1$, then P_A and $P_A{}'$ induce the same partition in $\Delta V_1V_2V_3$). The difference in appearance in the triangle would be in permutation of the triple (123) to (132) (derived from the subscripts of $V_{x_1}, V_{x_2}, V_{x_3}$ (Figure 4.4).

The number of possible distince P_A would depend upon the nature of the triangle $(V_1V_2V_3)$ under consideration:

i. If $V_1V_2V_3$ is a general triangle (Figure 4.5), then the intersections of the sets of lines

$$\{l_{x_i}, \quad i = 1, 2, 3 \mid l_{x_i} \| V_1V_3\}$$

$$\{l_{x_i}{}', \quad i = 1, 2, 3 \mid l_{x_i}{}' \| V_2V_3\}$$

$$\{l_{x_i}{}'', \quad i = 1, 2, 3 \mid l_{x_i}{}'' \| V_1V_2\}$$

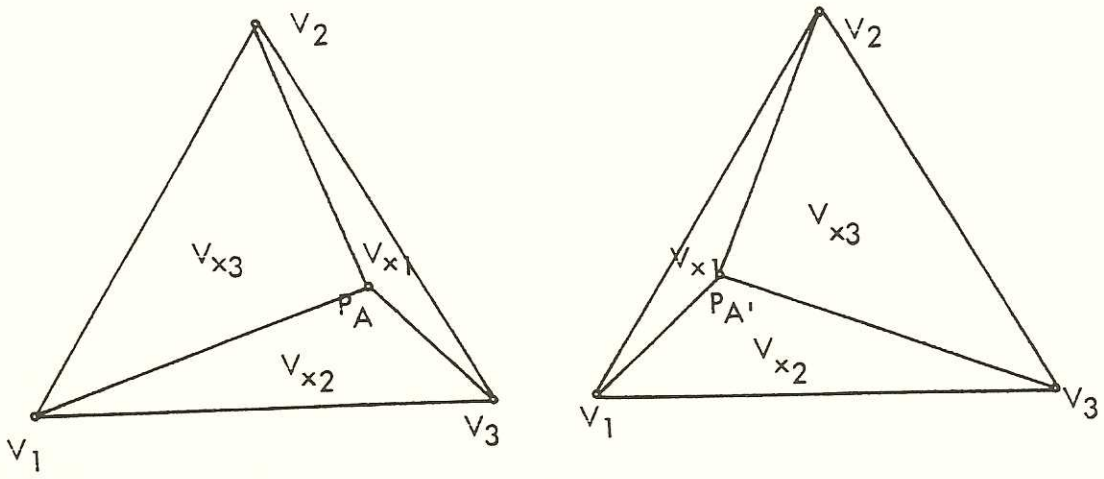

Figure 4.4

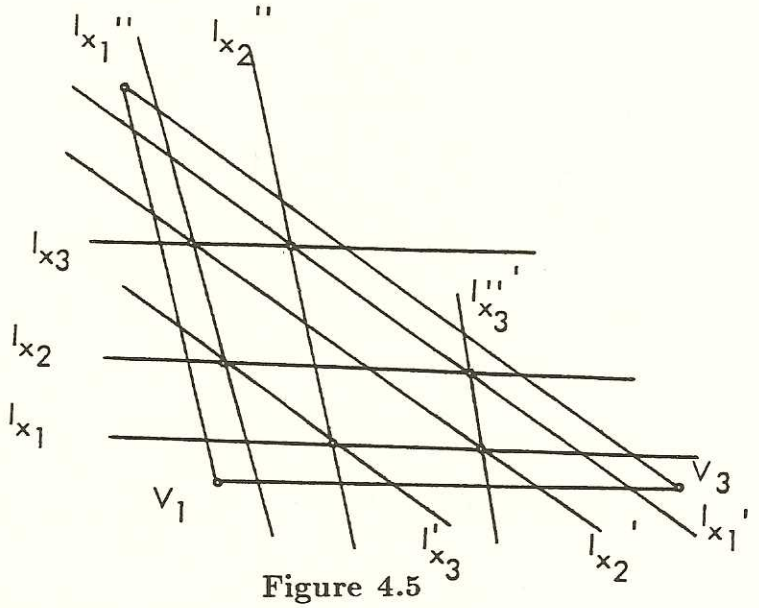

Figure 4.5

produce six distinct points $P_{A_1}, \ldots P_{A_6}$, given by

$$l_{x_1} \wedge l_{x_2}', \quad l_{x_1} \wedge l_{x_2}''$$

$$l_{x_2} \wedge l_{x_1}', \quad l_{x_2} \wedge l_{x_1}''$$

$$l_{x_1}' \wedge l_{x_2}'', \quad l_{x_1}'' \wedge l_{x_2}'$$

each of which satisfies the original conditions for P_A. Each $P_j \quad j = 1, \ldots, 6$ may produce a different set of $V_{x_i}, \quad i = 1, 2, 3$ such that

$$\text{area} V_{x_i} = \text{area} V_{x_i}' \quad i = 1, 2, 3,$$

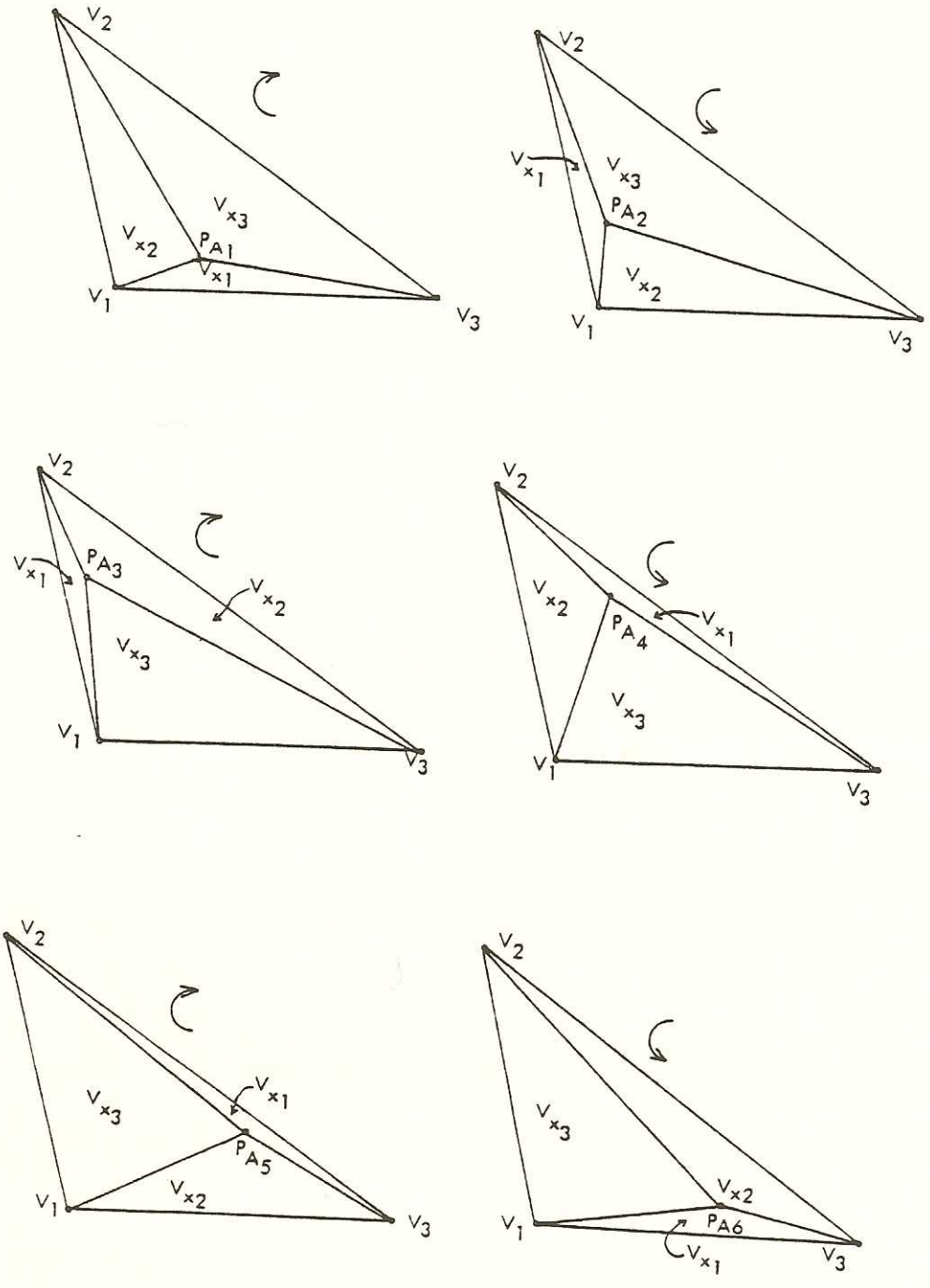

Figure 4.6

but V_{x_i} is not necessarily congruent to any of the $V_{x_i}{}'$. Then $P_{A_1}, P_{A_3}, P_{A_5}$ induce one orientation in the pattern of $V_{x_1}, V_{x_2}, V_{x_3}$ and $P_{A_2}, P_{A_4}, P_{A_6}$ induce the opposite orientation (Figure 4.6).

ii. If $\Delta V_1V_2V_3$ is isosceles, then the intersections of the appropriate sets of lines produce three points $P_{A_1}, P_{A_2}, P_{A_3}$ which are unique up to reflection of $\Delta V_1V_2V_3$ in its angle bisector through the third angle, while if $\Delta V_1V_2V_3$ is equilateral, the intersections of the appropriate sets of lines produce two points P_{A_1}, P_{A_2}, which are unique up to a central rotation of 120 degrees.

Partition with respect to perimeter

The smallest percentage of the perimeter that $\sum_{i=1}^{3} |V_iP|$, can represent occurs when P is the Steiner point (minimizing total shortest length from P (interior to the triangle) to each of the vertices of the triangle) of $\Delta V_1V_2V_3$.

1. Lower and upper bounds for the general sum $\sum_{i=1}^{3} |V_iP|$, can be determined as follows.

Let ρ denote the perimeter of $\Delta V_1V_2V_3$. Since S_p is within $\Delta V_1V_2V_3$, it follows that

$$|V_iS_p| + |V_jS_p| > |V_iV_j| \quad i \neq j; \quad i,j = 1,2,3.$$

2. Therefore, $2 \times \sum_{i=1}^{3} |V_iS_P| > \rho$ is a lower bound. Also, since P is within $\Delta V_1V_2V_3$, it follows that, for particular i, j, k

$$|V_iP| + |V_jP| < |V_iV_k| + |V_jV_k| \quad i \neq j \neq k$$

and similarly for other permutations of i, j, and k. Combining inequalities, it follows that

3. $2 \times \sum_{i=1}^{3} |V_iP| < 2 \times \rho$ is an upper bound. Combining the above inequalities with

$$\sum_{i=1}^{3} |V_iS_P| \leq \sum_{i=1}^{3} |V_iP|$$

gives

$$\rho < 2 \times \sum_{i=1}^{3} |V_iS_P| \leq 2 \times \sum_{i=1}^{3} |V_iP| < 2 \times \rho$$

Dividing by two throughout produces an upper bound for the general sum and also a lower bound for the Steiner network:

$$\rho/2 < \sum_{i=1}^{3} |V_iS_P| \leq \sum_{i=1}^{3} |V_iP| < \rho$$

Thus the total network length induced by P ranges between $\sum_{i=1}^{3} |V_i S_P|$ and a *least* upper bound $L_\rho < \rho$. In the Steiner problem, it is decided, *a priori*, to minimize this length. If, instead, the desired network length induced by P is chosen, *a priori* as X, where

$$\sum_{i=1}^{3} |V_i S_P| < X < L_\rho$$

then a set of network location problems similar to, but distinct from, finding networks has been formed.

Suppose it is desired that the internal perimeter of $\Delta V_i P V_j$ should contain $B_k\%$ of B, $i \neq j \neq k$; $i, j, k = 1, 2, 3$ where the B_k are determined *a priori* and $\sum_{k=1}^{3} B_k = 100$, and B is the length of the boundary of triangle $(V_1 V_2 V_3)$. (The internal perimeter of $\Delta V_i P V_j$ is the sum of the lengths of line segments $V_i P$ and $V_j P$.) The following procedure will determine a point P in the interior of $\Delta V_1 V_2 V_3$ such that

$\Delta V_{B_1} = \Delta V_2 P V_3$ has internal perimeter I_{B_1} containing $B_1\%$ of B

$\Delta V_{B_2} = \Delta V_1 P V_3$ has internal perimeter I_{B_2} containing $B_2\%$ of B

$\Delta V_{B_3} = \Delta V_1 P V_2$ has internal perimeter I_{B_3} containing $B_3\%$ of B

Existence of P; Figure 4.7

A triangle $(V_1 P V_3)$ with internal perimeter I_{B_2} and base $V_1 V_3$ is constructed by locating P_{B_2} at the intersection interior to $\Delta V_1 V_2 V_3$ of two circles each of which has radius of length $1/2B_2\%$ of B, one of which is centered at V_1 and the other at V_3. The internal perimeter of triangle $(V_1 P_{B_2} V_3)$ is $B_2\%$ of B, and, the locus of points described by P_{B_2} such that $V_1 V_3$ and B_2 are constant, is an ellipse e_{B_2} passing through P_{B_2} with foci at V_1 and V_3. The point P lies on e_{B_2}. A similar construction will yield a point P_{B_1} and an associated ellipse e_{B_1} with foci V_2 and V_3. Since P also must lie on e_{B_1}, the intersection of e_{B_1} and e_{B_2} is a location for the point P.

Enumeration of possibilities for P depends on the structure of $\Delta V_1 V_2 V_3$ and proceeds as in the previous section of this chapter.

Partition with respect to angle

The following procedure will determine a point P in the interior of $\Delta V_1 V_2 V_3$ such that

$$< V_2 P V_3 = (X_1/100)360$$

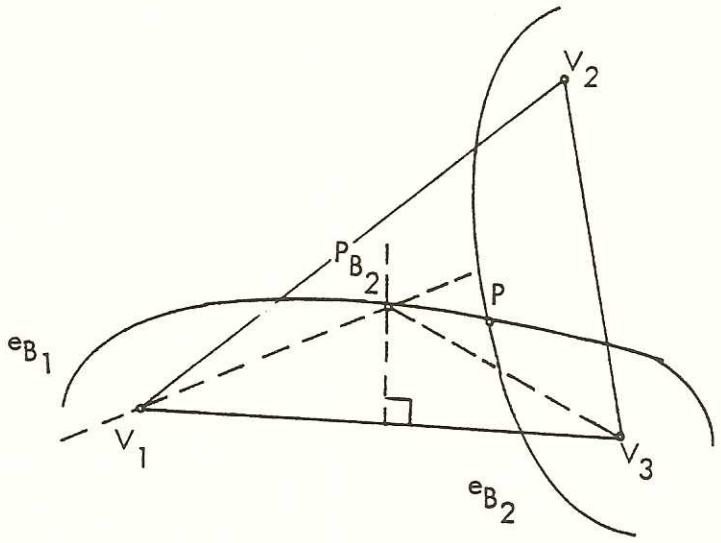

Figure 4.7

$$< V_1PV_3 = (X_2/100)360$$

$$< V_1PV_2 = (X_3/100)360$$

where $\sum_{i=1}^{3} X_i = 100$ (Figure 4.8).

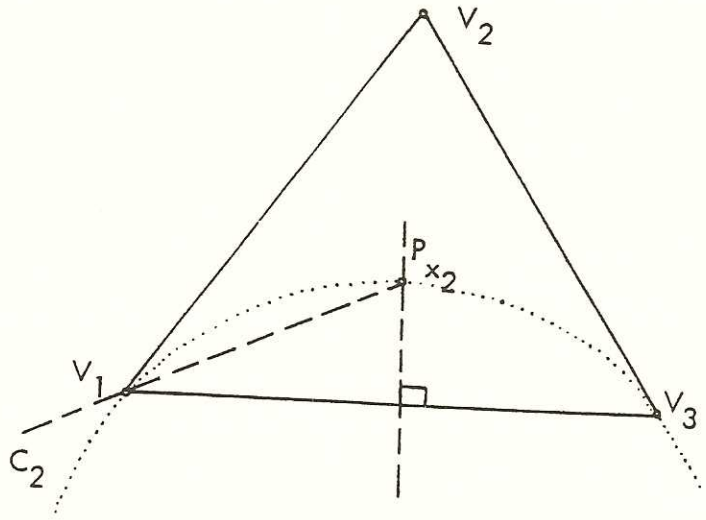

Figure 4.8

Locate a point P_{x_2} such that $< V_1P_{x_2}V_3 = (X_2/100)360$ where P_{x_2} lies on the perpendicular bisector of V_1V_3 and also on l_{v_1} where l passes through V_1 and forms an interior angle of $((180 - (X_2/100)360)/2)°$ with V_1V_3.

The locus of points P_{x_2} such that $< V_1P_{x_2}V_3$ is constant is the circumcircle C_2 about

$\Delta V_1 P_{x_2} V_3$. The point P must lie on C_2. Construction of a point P_{x_1} and of the circle C_1 passing through P_{x-1}, V_2, V_3 produces another circle on which P must lie. Thus the intersection of C_1 and C_2 interior to $\Delta V_1 V_2 V_3$ produces the required point P, and enumeration of possible locations for P depends on the structure of $\Delta V_1 V_2 V_3$ and proceeds as in the first section of this chapter.

This chapter has presented in detail, technique for determining the location of a point P within a triangle $V_1 V_2 V_3$ (with no angle less than or equal to 120 degrees) so that the set of sub-triangles formed along lines of partition of $\Delta V_1 V_2 V_3$ induced by P represent pre-assigned percentages of the areal, perimetric, or angular measure associated with $\Delta V_1 V_2 V_3$. Partitioning with respect to area might be used to emphasize the content of the space under consideration. Partitioning with respect to perimeter might be used to emphasize boundaries of, or, networks in, the space under consideration.

* This Chapter is based on material from S. Arlinghaus, "On Geographic Network Location Theory," Ph.D. Dissertation, Department of Geography, University of Michigan, 1977.

CHAPTER 5 *

An Enumeration of Candidate Steiner Networks

Algorithms for constructing Steiner networks, networks of shortest total length, rely on choosing the shortest network from a set of candidate networks, each a best possible form within particular topological constraints. To enumerate the number of possible candidates from which to choose the Steiner network, for a distribution of n points $V_1, \ldots V_n$ the number of separate types of topological classes will be counted. It will be assumed that the Steiner trees being counted are non-degenerate, that there are $(n-2)$ Steiner points $S_1, \ldots S_{n-2}$ in each, and that the $(n-2)$ spanning tree is of a particular topological type.

There are two different problems that can arise:

1. the $((n-2)$ spanning tree (Figure 5.1) may be hooked into the distribution of n points in a variety of distinct ways (Figure 5.2);

2. the sides of the polygon that are chosen to be rotated through 60 degrees may be selected in a variety of ways.

Figure 5.1

The procedure that follows will count the number of possible candidates with an $(n-2)$ spanning tree of given topological form that is hooked into the set of n vertices in a preassigned manner. These constraints would be specified by the spatial relations of the problem under consideration.

Proposition 5.1.

Suppose that:

1. $\mathcal{P}$ is a polygon with n vertices $V_1, \ldots V_n$;
2. n is an odd positive integer;
3. the $(n-2)$ spanning tree is linear in topological form; and,
4. the $(n-2)$ spanning tree is to be hooked into $\mathcal{P}$ in such a way that

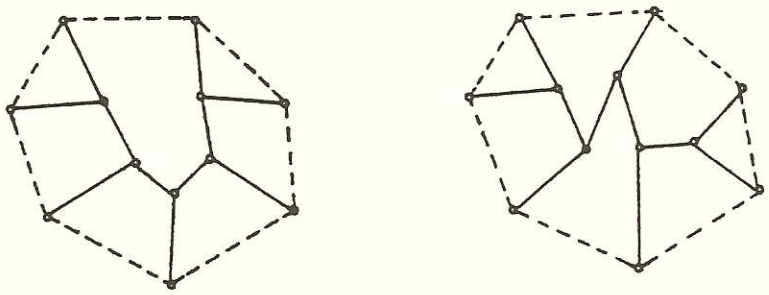

Figure 5.2

i. the two "small" triangles formed by connecting the two vertices of degree one of the linear $(n-2)$ spanning tree to $\mathcal{P}$ are separated by exactly one side of $\mathcal{P}$.

ii. no two edges linking vertices of degree 2 or the (n-2) spanning tree to $\mathcal{P}$ lie on opposite sides of the (n-2) spanning tree.

Then there are $n \times (n-2) \times (n-4) \times \ldots \times 5$ possible distinct candidates.

Proof:

There exist n different unordered pairs of sides of an n-gon with one side separating the two for if the sides of the n-gon are numbered clockwise, on alternate sides, then the desired set of unordered pairs is

$$\{(1,2),(2,3),\ldots,((n-1),n),(n,1)\}\text{(Figure 5.3)}$$

which has n elements.

For each of the n choices, there are $(n-2)$ choices at the next level and then $(n-4)$ for each of the $(n-2)$ and so on, down to 5 (there is only one S_p is a given triangle). Q.E.D.

Proposition 5.2

Suppose that:

1. P is a polygon with n vertices;
2. n is an even number, and
3. the $(n-2)$ spanning tree in P has maximal branching.

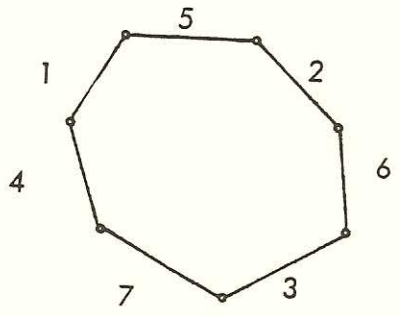

Figure 5.3

Then there are $n \times (m-2) \times (m-4) \times \ldots \times 5$ possible distinct networks where $m = n/2^{\alpha_0}$ and α_0 is the exponent representing the maximum number of 2's that can be factored out of n.

Proof.

Decompose n into the unique product of powers of prime factors, using the Fundamental Theorem of Arithmetic, as

$$n = 2^{\alpha_0} \times {p_1}^{\alpha_1} \times \cdots \times {p_r}^{\alpha_r},$$

p_i odd primes, α_i integers greater than or equal to 0, $\alpha_0 \neq 0$. The number of possible networks is

$$2^{\alpha_0} \times m \times (m-2) \times (m-4) \times \cdots \times 5$$

where $m = (n/2^{\alpha_0})$, for there are two choices for ways to select alternate sides as long as n is divisible by two (α_0 times), and, then we are left with a polygon with an odd number of sides; that is, one with ${p_1}^{\alpha_1} \times {p_2}^{\alpha_2} \times \cdots \times {p_r}^{\alpha_r}$ sides. Then count the rest of the networks using Proposition 5.1, yielding the above formula which may be rewritten

$$n \times (m-2) \times (m-4) \times \cdots \times 5.$$

Q.E.D.

The hypotheses of these two propositions are highly restrictive. This fact suggests that if geographic constraints impose the restrictions in a natural way in a given problem, then,

for example, the figure of 105 possible topologies for 6 vertices and 4 Steiner points, cited by Gilbert and Pollack [1968], can be reduced to six possibilities using Proposition 5.2.

Definition.

The following construction will associate a number, called "3-length," with each vertex V_i of a convex polygon (Figure 5.4).

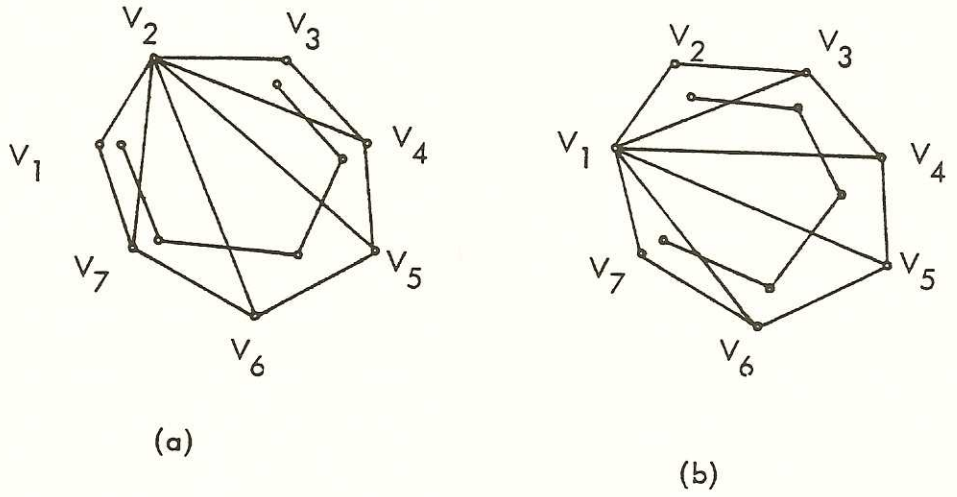

Figure 5.4

Connect vertex V_i to every point of the polygon, creating a partition of the polygon into $(n-2)$ triangles. Find the Steiner point of each of these $(n-2)$ triangles; link these together and measure the length, giving the 3-length associated with V_i.

Conjecture.

In a polygon $\mathcal{P}$ with an odd number of sides, the minimal second level Steiner candidate network of a topological type that exhibits bilateral rather than radial symmetry will have a vertex of degree one that is incident with an axis of symmetry located at that vertex of $\mathcal{P}$ with which minimal 3-length is associated. (There should be an extension of this to even numbers that are not congruent to 1(mod 3) and to even numbers that are not of the form $3 \times 2^{\alpha_0}$).

* This Chapter is based on material from S. Arlinghaus, "On Geographic Network Location Theory," Ph.D. Dissertation, Department of Geography, University of Michigan, 1977.

CHAPTER 6 *

A Topological Generation Gap

Point set topology offers interesting ways to capture qualitative real-world concepts that are not usually characterized using mathematics (Arlinghaus, 1986). The "open set" is fundamental to point-set topology; loosely, an open set might be viewed as a disc without a circular boundary. Choose a point within the disc–no matter how close one gets to the boundary, there is always some smaller disc that can be centered on the selected point and yet remain within the larger disc. There is a uniformity to the open set; thus, it might be regarded as an abstract ideal for a geographically uniform region.

The definition of a "topology" is given below. Note that most geographic works employ the word topology to refer to some sort of connection pattern linking a set of locations. This conventional usage is, at best, weak; it does not generally address any of the fundamental issues required–such as what are the open sets and what are the relationships between subsets of open sets.

Definition 6.1 (after Kelley and Mansfield).

Let X be a non-empty set and let $\mathcal{T}$ be any collection of subsets of X. Then the collection $\mathcal{T}$ is a *topology* for X:

a. if $X \in \mathcal{T}$ and $\phi \in \mathcal{T}$

b. if $G_\lambda \in \mathcal{T}$ for all $\lambda \in \Lambda$, it follows that $\bigcup_{\lambda \in \Lambda} \in \mathcal{T}$. That is, arbitrary unions of elements of $\mathcal{T}$ are once again elements of $\mathcal{T}$.

c. if $G_1, G_2, \ldots, G_n \in \mathcal{T}$ and $n \in \mathcal{Z}^+$, it follows that $\bigcap_{i=1}^{n} \in \mathcal{T}$. Finite intersections of elements of $\mathcal{T}$ are once again elements of $\mathcal{T}$.

The members of $\mathcal{T}$ that satisfy these conditions are *open* sets; thus, a topology on a set X is a collection of subsets chosen so that the whole set itself and the empty set are members of the topology and so that unions of an arbitrary number of subsets in the topology are also in the topology, and so that finite intersections of members of the topology are in the topology as well. Loosely speaking, the topology offers a sort of a closed system on the underlying set, within which much interaction can occur.

The example below shows why there is a need for the *finiteness* characteristic associated with intersections stated in part c. of Definition 6.1.

Let $X = [0, 1)$, the half-open interval that includes 0 as one endpoint but does not include 1 at the other end.

Let $\mathcal{T} = \{[0, \frac{1}{n}) \mid n \in \mathcal{Z}^+\} \cup \phi$.

a. $\phi \in \mathcal{T}$; $X \in \mathcal{T}$ since 1 is a positive integer and $[0, \frac{1}{1}) = [0, 1) \in \mathcal{T}$.

b. the union of any collection of right-half open intervals, from $\mathcal{T}$, is again right-half open and has 0 as the left-hand endpoint.

c. finite intersections of right-half open intervals from $\mathcal{T}$ are once again right-half open intervals and have 0 as left-hand end; however, an infinite intersection would yield

$$\bigcap_{n \in \mathcal{Z}} [0, \frac{1}{n}) = \{0\} \notin \mathcal{Z}$$

Because the set whose single element is 0 is not a member of the topology, this infinite intersection is not a member of the topology; hence, the reason for the finite intersection property.

Definition 6.2 (after Kelley and Mansfield)

If $\mathcal{T}$ is a topology for the set X, then the pair $(X, \mathcal{T})$ is called a *topological space*, and, as noted, the sets of $\mathcal{T}$ are called the *open* sets of $\mathcal{T}$.

Definition 6.3–(after Mansfield)

A subset F of X is closed relative to $\mathcal{T}$ if and only if the complement of F (all elements of X **not** in F) is one of the open sets of $\mathcal{T}$.

Definition 6.4–(after Mansfield)

Within the set of real numbers with a topology of open intervals as open sets, a nonempty subset is *bounded* if it is both bounded above (there is an upper bound larger than or equal to all members) and if it is bounded below.

Heine-Borel Theorem (after Taylor)

Let S be a bounded and closed point set, and let S be covered by a collection of open sets, $\mathcal{T}$. Then a finite number of open sets may be chosen from the collection in such a way that S is covered by the new finite collection.

Let S = {set of all human beings}; an element of S is closed since it contains its own boundary, and so since there are a finite number of human beings, the union S of a finite number of closed sets is also closed. Also S is bounded by the planet.

Let $\mathcal{T} = \{\text{all views of the world}\}$. This set has an infinite number of elements, covering all possible human situations.

Select a finite set T_1 from $\mathcal{T}$; if T_1 covers S (i.e., if the Heine-Borel theorem holds), this forms a set of values from which members of S may draw, and produces "rational" behavior. If the set T_1 does not cover S (i.e., if the Heine-Borel theorem does not hold) no world view is available at some points and this produces "irrational" behavior. The intersection of sets from $\mathcal{T}$ produces areas of conformity.

Suppose S is the Cantor set of the excluded middle. The idea of this set can be expressed as follows. Take the closed interval from 0 to 1. First, partition it into thirds and throw away the open middle interval. Next, use each of the two remaining "offspring" closed intervals and repeat the procedure. Repeat the procedure indefinitely, through successive levels of "offspring" intervals, yielding the "Cantor" set (Kelley, p. 165). This set, S, is closed and bounded. But it cannot be covered by a collection of open sets. If the manner in which this set is formed is viewed as a sequence of generations, then the failure of the Heine-Borel theorem on this set may be likened to the failure to be able to cover the "generation gap" with a set of values compatible with both ends of this gap.

* Based on unpublished material by the author from 1974-76.

REFERENCES

Arlinghaus, S., *Essays on Mathematical Geography–I*, Ann Arbor: Institute of Mathematical Geography, Monograph Series #3, 1986.

Kelley, J. L., *General Topology*, Princeton: D. Van Nostrand, 1955, 1963.

Mansfield, M. J., *Introduction to Topology*, Princeton: D. Van Nostrand, 1963.

Taylor, A. E., *Advanced Calculus*, Boston: Ginn and Co., 1955.

CHAPTER 7 *

Synthetic Centers of Gravity: Conjecture

The center of gravity of a triangle is the point of intersection of the medians (line joining a vertex to the midpoint of the opposite side) of the triangle. For higher levels of polygons, the integral calculus supplies methods for finding the center of gravity. Calculus methods require the introduction of coordinates which may not be desirable. The construction below offers a way to find the center of gravity for a convex polygon; it is presented as an open conjecture, because the construction has not yet been proved (or disproved). It appears that the following synthetic construction, expressed in terms of a couple of examples, will generalize.

1. Given a quadrilateral $A_1A_2A_3A_4$ (Figure 7.1); partition the quadrilateral into two triangles, $A_1A_2A_4$ and $A_1A_3A_4$ (Figure 7.1). Find the centers of gravity, G_1 and G_2, of each of these triangles (Figure 7.1).

2. Connect the centers of gravity G_1 and G_2.

Conjecture. The center of gravity of $A_1A_2A_3A_4$ lies on the line joining G_1 and G_2 (Figure 7.1).

3. Repartition the given quadrilateral into triangles $A_1A_2A_3$ and $A_2A_3A_4$. Find the centers of gravity, G_3 and G_4, of each of these triangles and join them with a line (Figure 7.2).

4. Superimpose the two different partitions. Using the conjecture, since the center of gravity G of the quadrilateral must lie on the line G_1G_2 and on the line G_3G_4. Thus, G is the intersection point of these two lines (Figure 7.3) and the center of gravity of the quadrilateral has been determined.

5. To find the center of gravity of a higher order polygon using this procedure is again quite simple, requiring one dissection of the higher order n-gon into a triangle and an $n-1$-gon followed by another dissection of the n-gon into a different triangle and $n-1$-gon. Iteration finds the needed location in the $n-1$-gons, reducing them through successive dissection to a triangle.

6. Thus, consider the pentagon $A_1A_2A_3A_4A_5$ (Figure 7.4). Dissect it into a triangle $A_1A_4A_5$ and a quadrilateral $A_1A_2A_3A_4$. Find the center of gravity G_1 of the triangle, and

find the center of gravity G_2 of the quadrilateral using the strategy in steps 1 to 4 above. Join G_1 and G_2 (Figure 7.4). The conjecture says that the center of gravity lies on this line.

7. Repartition the pentagon into the triangle $A_2A_3A_4$ and the quadrilateral $A_1A_2A_4A_5$, and find their respective centers of gravity, G_3 and G_4. Join the two centers of gravity (Figure 7.5); the center of gravity of the pentagon lies along this line.

8. Superimpose Figures 7.4 and 7.5; the center of gravity lies on lines G_1G_2 and on G_3G_4 (Figure 7.6). Thus, the intersection of these two lines is the center of gravity, G, of the pentagon.

Open questions

Prove or disprove the conjecture; prove or disprove the construction; and, independent of the outcome of establishing the validity of the conjecture, determine sets of circumstances in which it is important to be able to find centers of gravity without calculus techniques (perhaps in a digital mapping environment).

* Based on unpublished work of the author from 1973.

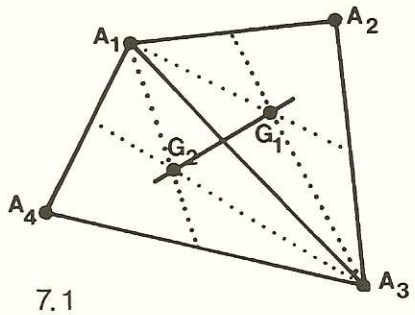

7.1

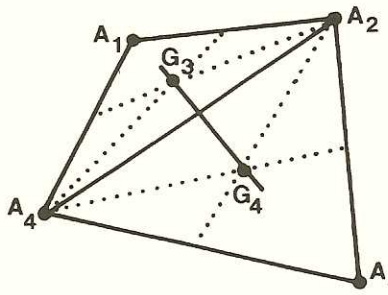

7.2

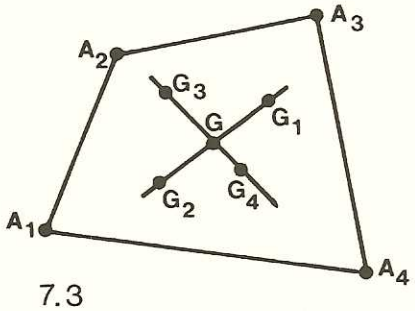

7.3

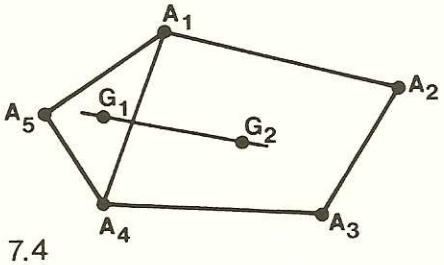

7.4

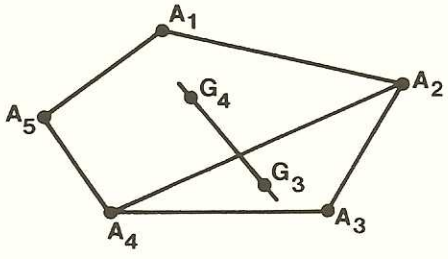

7.5

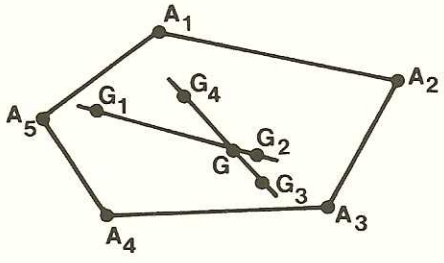

7.6

Figures 7.1 to 7.6. 7.1: Centers of gravity of two triangles and the line joining them. 7.2: Centers of gravity of two triangles and the line joining them. 7.3: Superimposition of 7.1 and 7.2–the center of gravity of the quadrilateral is shown as the intersection of the two lines. 7.4: Centers of gravity of a triangle and a quadrilateral and the line joining them. 7.5: Centers of gravity of another triangle and a quadrilateral and the line joining them. 7.6: Superimposition of 7.4 and 7.5– the center of gravity of the pentagon is shown as the intersection of the two lines.

CATALOGUE, 1991

INSTITUTE OF MATHEMATICAL GEOGRAPHY (IMaGe)
2790 BRIARCLIFF
ANN ARBOR, MI 48105-1429; U.S.A.
(313) 761-1231; IMaGe@UMICHUM

"Imagination is more important than knowledge"
A. Einstein

MONOGRAPH SERIES

Scholarly Monographs–Original Material
All monographs are $15.95, except #12 which is $39.95

Exclusive of shipping and handling; prices listed and payable in U.S. funds on a U.S. bank, only.

Monographs are printed by **Digicopy** on 100% recycled paper of archival quality.

1. Sandra L. Arlinghaus and John D. Nystuen. *Mathematical Geography and Global Art: the Mathematics of David Barr's "Four Corners Project,"* 1986.

This monograph contains Nystuen's calculations, actually used by Barr to position his abstract tetrahedral sculpture within the earth. Placement of the sculpture vertices in Easter Island, South Africa, Greenland, and Indonesia was chronicled in film by The Archives of American Art for The Smithsonian Institution. In addition to the archival material, this monograph also contains Arlinghaus's solutions to broader theoretical questions–was Barr's choice of a tetrahedron unique within his initial constraints, and, within the set of Platonic solids?

2. Sandra L. Arlinghaus. *Down the Mail Tubes: the Pressured Postal Era, 1853-1984*, 1986.

The history of the pneumatic post, in Europe and in the United States, is examined for the lessons it might offer to the technological scenes of the late twentieth century. As Sylvia L. Thrupp, Alice Freeman Palmer Professor Emeritus of History, The University of Michigan, commented in her review of this work "Such brief comment does far less than justice to the intelligence and the stimulating quality of the author's writing, or to the breadth of her reading. The detail of her accounts of the interest of American private enterprise, in New York and other large cities on this continent, in pushing for construction of large tubes in systems to be leased to the government, brings out contrast between American and European views of how the new technology should be managed. This and many other sections of the monograph will set readers on new tracks of thought."

3. Sandra L. Arlinghaus. *Essays on Mathematical Geography*, 1986.

A collection of essays intended to show the range of power in applying pure mathematics to human systems. There are two types of essay: those which employ traditional mathematical proof, and those which do not. As mathematical proof may itself be regarded as art, the former style of essay might represent "traditional" art, and the latter, "surrealist" art. Essay titles are: "The well-tempered map projection," "Antipodal graphs," "Analogue clocks," "Steiner transformations," "Concavity and urban settlement patterns," "Measuring the vertical city," "Fad and permanence in human systems," "Topological exploration in geography," "A space for thought," and "Chaos in human systems–the Heine-Borel Theorem."

4. Robert F. Austin, *A Historical Gazetteer of Southeast Asia*, 1986.

Dr. Austin's Gazetteer draws geographic coordinates of Southeast Asian place-names together with references to these place-names as they have appeared in historical and literary documents. This book is of obvious use to historians and to historical geographers specializing in Southeast Asia. At a deeper level, it might serve as a valuable source in establishing place-name linkages which have remained previously unnoticed, in documents describing trade or other communications connections, because of variation in place-name nomenclature.

5. Sandra L. Arlinghaus, *Essays on Mathematical Geography–II*, 1987.

Written in the same format as IMaGe Monograph #3, that seeks to use "pure" mathematics in real-world settings, this volume contains the following material: "Frontispiece–the Atlantic Drainage Tree," "Getting

a Handel on Water-Graphs," "Terror in Transit: A Graph Theoretic Approach to the Passive Defense of Urban Networks," "Terrae Antipodum," "Urban Inversion," "Fractals: Constructions, Speculations, and Concepts," "Solar Woks," "A Pneumatic Postal Plan: The Chambered Interchange and ZIPPR Code," "Endpiece."

6. Pierre Hanjoul, Hubert Beguin, and Jean-Claude Thill, *Theoretical Market Areas Under Euclidean Distance*, 1988. (English language text; Abstracts written in French and in English.)

Though already initiated by Rau in 1841, the economic theory of the shape of two-dimensional market areas has long remained concerned with a representation of transportation costs as linear in distance. In the general gravity model, to which the theory also applies, this corresponds to a decreasing exponential function of distance deterrence. Other transportation cost and distance deterrence functions also appear in the literature, however. They have not always been considered from the viewpoint of the shape of the market areas they generate, and their disparity asks the question whether other types of functions would not be worth being investigated. There is thus a need for a general theory of market areas: the present work aims at filling this gap, in the case of a duopoly competing inside the Euclidean plane endowed with Euclidean distance.

(Bien qu'ébauchée par Rau dès 1841, la théorie économique de la forme des aires de marché planaires s'est longtemps contentée de l'hypothèse de coûts de transport proportionnels à la distance. Dans le modèle gravitaire généralisé, auquel on peut étendre cette théorie, ceci correspond au choix d'une exponentielle décroissante comme fonction de dissuasion de la distance. D'autres fonctions de coût de transport ou de dissuasion de la distance apparaissent cependant dans la littérature. La forme des aires de marché qu'elles engendrent n'a pas toujours été étudiée ; par ailleurs, leur variété amène à se demander si d'autres fonctions encore ne mériteraient pas d'être examinées. Il paraît donc utile de disposer d'une théorie générale des aires de marché : ce à quoi s'attache ce travail en cas de duopole, dans le cadre du plan euclidien muni d'une distance euclidienne.)

7. Keith J. Tinkler, Editor, *Nystuen—Dacey Nodal Analysis*, 1988.

Professor Tinkler's volume displays the use of this graph theoretical tool in geography, from the original Nystuen—Dacey article, to a bibliography of uses, to original uses by Tinkler. Some reprinted material is included, but by far the larger part is of previously unpublished material. (Unless otherwise noted, all items listed below are previously unpublished.) Contents: " 'Foreward' " by Nystuen, 1988; "Preface" by Tinkler, 1988; "Statistics for Nystuen—Dacey Nodal Analysis," by Tinkler, 1979; Review of Nodal Analysis literature by Tinkler (pre–1979, reprinted with permission; post—1979, new as of 1988); FORTRAN program listing for Nodal Analysis by Tinkler; "A graph theory interpretation of nodal regions" by John D. Nystuen and Michael F. Dacey, reprinted with permission, 1961; Nystuen—Dacey data concerning telephone flows in Washington and Missouri, 1958, 1959 with comment by Nystuen, 1988; "The expected distribution of nodality in random (p, q) graphs and multigraphs," by Tinkler, 1976.

8. James W. Fonseca, *The Urban Rank–size Hierarchy: A Mathematical Interpretation*, 1989.

The urban rank–size hierarchy can be characterized as an equiangular spiral of the form $r = ae^{\theta \cot \alpha}$. An equiangular spiral can also be constructed from a Fibonacci sequence. The urban rank–size hierarchy is thus shown to mirror the properties derived from Fibonacci characteristics such as rank–additive properties. A new method of structuring the urban rank–size hierarchy is explored which essentially parallels that of the traditional rank–size hierarchy below rank 11. Above rank 11 this method may help explain the frequently noted concavity of the rank–size distribution at the upper levels. The research suggests that the simple rank–size rule with the exponent equal to 1 is not merely a special case, but rather a theoretically justified norm against which deviant cases may be measured. The spiral distribution model allows conceptualization of a new view of the urban rank–size hierarchy in which the three largest cities share functions in a Fibonacci hierarchy.

9. Sandra L. Arlinghaus, *An Atlas of Steiner Networks*, 1989.

A Steiner network is a tree of minimum total length joining a prescribed, finite, number of locations; often new locations are introduced into the prescribed set to determine the minimum tree. This Atlas explains the mathematical detail behind the Steiner construction for prescribed sets of n locations and displays the

steps, visually, in a series of Figures. The proof of the Steiner construction is by mathematical induction, and enough steps in the early part of the induction are displayed completely that the reader who is well–trained in Euclidean geometry, and familiar with concepts from graph theory and elementary number theory, should be able to replicate the constructions for full as well as for degenerate Steiner trees.

10. Daniel A. Griffith, *Simulating $K = 3$ Christaller Central Place Structures: An Algorithm Using A Constant Elasticity of Substitution Consumption Function*, 1989.

An algorithm is presented that uses BASICA or GWBASIC on IBM compatible machines. This algorithm simulates Christaller $K = 3$ central place structures, for a four–level hierarchy. It is based upon earlier published work by the author. A description of the spatial theory, mathematics, and sample output runs appears in the monograph. A digital version is available from the author, free of charge, upon request; this request must be accompanied by a 5.5–inch formatted diskette. This algorithm has been developed for use in Social Science classroom laboratory situations, and is designed to (a) cultivate a deeper understanding of central place theory, (b) allow parameters of a central place system to be altered and then graphic and tabular results attributable to these changes viewed, without experiencing the tedium of massive calculations, and (c) help promote a better comprehension of the complex role distance plays in the space–economy. The algorithm also should facilitate intensive numerical research on central place structures; it is expected that even the sample simulation results will reveal interesting insights into abstract central place theory.

The background spatial theory concerns demand and competition in the space–economy; both linear and non–linear spatial demand functions are discussed. The mathematics is concerned with (a) integration of non–linear spatial demand cones on a continuous demand surface, using a constant elasticity of substitution consumption function, (b) solving for roots of polynomials, (c) numerical approximations to integration and root extraction, and (d) multinomial discriminant function classification of commodities into central place hierarchy levels. Sample output is presented for contrived data sets, constructed from artificial and empirical information, with the wide range of all possible central place structures being generated. These examples should facilitate implementation testing. Students are able to vary single or multiple parameters of the problem, permitting a study of how certain changes manifest themselves within the context of a theoretical central place structure. Hierarchical classification criteria may be changed, demand elasticities may or may not vary and can take on a wide range of non–negative values, the uniform transport cost may be set at any positive level, assorted fixed costs and variable costs may be introduced, again within a rich range of non–negative possibilities, and the number of commodities can be altered. Directions for algorithm execution are summarized. An ASCII version of the algorithm, written directly from GWBASIC, is included in an appendix; hence, it is free of typing errors.

11. Sandra L. Arlinghaus and John D. Nystuen, *Environmental Effects on Bus Durability*, 1990.

This monograph draws on the authors' previous publications on "Climatic" and "Terrain" effects on bus durability. Material on these two topics is selected, and reprinted, from three published papers that appeared in the *Transportation Research Record* and in the *Geographical Review*. New material concerning "congestion" effects is examined at the national level, to determine "dense," "intermediate," and "sparse" classes of congestion, and at the local level of congestion in Ann Arbor (as suggestive of how one might use local data). This material is drawn together in a single volume, along with a summary of the consequences of all three effects simultaneously, in order to suggest direction for more highly automated studies that should follow naturally with the release of the 1990 U. S. Census data.

12. Daniel A. Griffith, Editor. *Spatial Statistics: Past, Present, and Future*, 1990.

Proceedings of a Symposium of the same name held at Syracuse University in Summer, 1989. Content includes a Preface by Griffith and the following papers:

Brian Ripley, "Gibbsian interaction models";
J. Keith Ord, "Statistical methods for point pattern data";
Luc Anselin, "What is special about spatial data";
Robert P. Haining, "Models in human geography:
problems in specifying, estimating, and validating models for spatial data";
R. J. Martin, "The role of spatial statistics in geographic modelling";
Daniel Wartenberg, "Exploratory spatial analyses: outliers, leverage points, and influence functions";

J. H. P. Paelinck, "Some new estimators in spatial econometrics";
Daniel A. Griffith, "A numerical simplification for estimating parameters of spatial autoregressive models";
Kanti V. Mardia "Maximum likelihood estimation for spatial models";
Ashish Sen, "Distribution of spatial correlation statistics";
Sylvia Richardson, "Some remarks on the testing of association between spatial processes";
Graham J. G. Upton, "Information from regional data";
Patrick Doreian, "Network autocorrelation models: problems and prospects."

Each chapter is preceded by an "Editor's Preface" and followed by a Discussion and, in some cases, by an author's Rejoinder to the Discussion.

13. Sandra L. Arlinghaus, Editor. *Solstice—I*, 1990.

William Kingdon Clifford, Reprint of "Postulates of the science of space";

Sandra L. Arlinghaus, "Beyond the fractal";

William C. Arlinghaus, "Groups, graphs, and God";

John D. Nystuen, Reprint of "A City of strangers: Spatial aspects of alienation in the Detroit metropolitan region";

Sandra L. Arlinghaus, "Scale and dimension: Their logical harmony";

Sandra L. Arlinghaus, "Parallels between parallels";

Sandra L. Arlinghaus, William C. Arlinghaus, and John D. Nystuen, "The Hedetniemi matrix sum: A real–world application";

Sandra L. Arlinghaus, "Fractal geometry of infinite pixel sequences: 'Super–definition' resolution?";

SOLSTICE: AN ELECTRONIC JOURNAL OF GEOGRAPHY AND MATHEMATICS
Founding Editor, Sandra L. Arlinghaus
Director, IMaGe
Volume I, number 1, Summer 1990
Volume I, number 2, Winter 1990
Volume II, number 1, Summer 1990

Solstice is geography's first electronic journal. Articles are typeset using TEX so that mathematical notation, as well as usual text, may be transmitted as an ASCII file to individuals requesting copies of *Solstice*. The electronic file is transmitted, free of charge, across the bitnet network. Individuals wishing hard copy obtain it by downloading the electronic TEX file at their own expense to produce typeset copy on the equipment of their university. Because exactly the number of copies desired are produced, this is an environmentally-aware method of producing journals; it is also extremely inexpensive, particularly for mathematical typesetting.

Because the capability to transmit photos and other graphics is not yet available, individuals wishing to have the complete document may purchase it from IMaGe at a cost of $15.95 per year. The two copies per year (mailed on e-mail at (or near) the precise times of the Summer and Winter astronomical solstices) are downloaded on a Xerox 9700 at The University of Michigan (on a special account for *Solstice*) and placed in the on-demand monograph series of IMaGe–also an environmentally-sound publication procedure.

DISCUSSION PAPERS–ORIGINAL

Editor, Daniel A. Griffith
Professor of Geography
Syracuse University

Founder as an IMaGe series: Sandra L. Arlinghaus

1. *Spatial Regression Analysis on the PC: Spatial Statistics Using Minitab.* 1989. $12.95.

DISCUSSION PAPERS–REPRINTS

Editor, John D. Nystuen

Professor of Geography and Urban Planning

The University of Michigan

Founder as an IMaGe series: Sandra L. Arlinghaus

1. *Reprint of the Papers of the Michigan InterUniversity Community of Mathematical Geographers.* Editor, John D. Nystuen. Entire volume of twelve papers: $39.95.

Contents–original editor: John D. Nystuen.

1. Arthur Getis, "Temporal land use pattern analysis with the use of nearest neighbor and quadrat methods." July, 1963

2. Marc Anderson, "A working bibliography of mathematical geography." September, 1963.

3. William Bunge, "Patterns of location." February, 1964.

4. Michael F. Dacey, "Imperfections in the uniform plane." June, 1964.

5. Robert S. Yuill, A simulation study of barrier effects in spatial diffusion problems." April, 1965.

6. William Warntz, "A note on surfaces and paths and applications to geographical problems." May, 1965.

7. Stig Nordbeck, "The law of allometric growth." June, 1965.

8. Waldo R. Tobler, "Numerical map generalization;" and Waldo R. Tobler, "Notes on the analysis of geographical distributions." January, 1966.

9. Peter R. Gould, "On mental maps." September, 1966.

10. John D. Nystuen, "Effects of boundary shape and the concept of local convexity;" Julian Perkal, "On the length of empirical curves;" and Julian Perkal, "An attempt at objective generalization." December, 1966.

11. E. Casetti and R. K. Semple, "A method for the stepwise separation of spatial terends." April, 1968.

12. W. Bunge, R. Guyot, A. Karlin, R. Martin, W. Pattison, W. Tobler, S. Toulmin, and W. Warntz, "The philosophy of maps." June, 1968.

Reprints of out-of-print textbooks.
Printer and obtainer of copyright permission: Digicopy
Inquire for cost of reproduction—include class size

1. Allen K. Philbrick. This Human World.

Publications of the Institute of Mathematical Geography have been reviewed in

1. *The Professional Geographer* published by the Association of American Geographers;
2. *The Urban Specialty Group Newsletter* of the Association of American Geographers;
3. *Mathematical Reviews* published by the American Mathematical Society;
4. *The American Mathematical Monthly* published by the Mathematical Association of America;
5. *Zentralblatt* Springer-Verlag, Berlin
6. *Mathematics Magazine* , published by the Mathematical Association of America.